Causes and Consequences of Genetic Background Effects Illuminated by Integrative Genomic Analysis

Christopher H. Chandler,*,†,1,2 Sudarshan Chari,*,† David Tack,*,3 and Ian Dworkin*,†,1
*Michigan State University, Department of Zoology, East Lansing, Michigan, 48824, and †BEACON Center for the Study of Evolution in Action

ABSTRACT The phenotypic consequences of individual mutations are modulated by the wild-type genetic background in which they occur. Although such background dependence is widely observed, we do not know whether general patterns across species and traits exist or about the mechanisms underlying it. We also lack knowledge on how mutations interact with genetic background to influence gene expression and how this in turn mediates mutant phenotypes. Furthermore, how genetic background influences patterns of epistasis remains unclear. To investigate the genetic basis and genomic consequences of genetic background dependence of the *scalloped*^{E3} allele on the *Drosophila melanogaster* wing, we generated multiple novel genome-level datasets from a mapping-by-introgression experiment and a tagged RNA gene expression dataset. In addition we used whole genome resequencing of the parental lines—two commonly used laboratory strains—to predict polymorphic transcription factor binding sites for SD. We integrated these data with previously published genomic datasets from expression microarrays and a modifier mutation screen. By searching for genes showing a congruent signal across multiple datasets, we were able to identify a robust set of candidate loci contributing to the background-dependent effects of mutations in *sd*. We also show that the majority of background-dependent modifiers previously reported are caused by higher-order epistasis, not quantitative noncomplementation. These findings provide a useful foundation for more detailed investigations of genetic background dependence in this system, and this approach is likely to prove useful in exploring the genetic basis of other traits as well.

GENETICISTS often strictly control their organisms' wild-type genetic backgrounds when experimentally dissecting genetic pathways. Although this tight control is necessary to avoid faulty inferences caused by confounding variables (*e.g.*, Burnett *et al.* 2011), it can often paint an incomplete or even incorrect picture; no genetic pathway or network exists in a vacuum. Instead, these networks occur in the context of all the alleles in the genome, which usually vary among individuals. There is substantial evidence that wild-type genetic background almost always modulates the phenotypic effects of mutations (*e.g.*, McKenzie *et al.* 1982; Threadgill *et al.* 1995; Atallah *et al.* 2004; Milloz *et al.* 2008; Chandler 2010; Dowell *et al.* 2010; Gerke *et al.* 2010). The influence of wild-type genetic backgrounds also extends to interactions among mutations (Remold and Lenski 2004; Dworkin *et al.* 2009; Wang *et al.* 2013b), altering patterns of epistasis, and these complex interactions are likely widespread (Chari and Dworkin 2013). Alleles that influence many mutant phenotypes segregate in most natural populations, representing a potential source of cryptic genetic variation (Polaczyk *et al.* 1998; Félix 2007; Vaistij *et al.* 2013). In many cases, this cryptic variation has been described phenomenologically, or via the partitioning of genetic variance components (Gibson *et al.* 1999; Dworkin *et al.* 2003; McGuigan *et al.* 2011). However, its genetic basis remains poorly understood (Dworkin *et al.* 2003; Duveau and Félix 2012).

If our aim is to understand how a specific perturbation to a genetic network (*e.g.*, a particular mutation) influences the phenotype outside a laboratory setting—a goal shared by

doi: 10.1534/genetics.113.159426
Manuscript received November 7, 2013; accepted for publication January 28, 2014; published Early Online February 5, 2014.
Supporting information is available online at http://www.genetics.org/lookup/suppl/doi:10.1534/genetics.113.159426/-/DC1.
Data deposited in the Dryad Repository, doi:10.5061/dryad.1375s. NCBI SRA: SRP035237, SRX423326, SRX423475, SRX423855, SRX423874, SRX424394, SRX424397, SRX424398.
[1]Corresponding authors: Department of Zoology, Michigan State University, East Lansing, MI 48824. E-mail: idworkin@msu.edu; and Department of Biological Sciences, SUNY Oswego, Oswego, New York 13126. E-mail: christopher.chandler@oswego.edu
[2]Present address: Department of Biological Sciences, SUNY Oswego, Oswego, New York 13126.
[3]Present address: University of British Columbia, Centre for Plant Research, Vancouver, BC, Canada, V6T 1Z4.

multiple disciplines, from the genetics of disease to evolutionary biology—then we must go beyond simply characterizing the phenotypic consequences of background-dependent effects. That is, we need to understand both the causes and consequences of this genetic background dependence of mutational effects (Chandler *et al.* 2013). For instance, one study showed that specific quantitative trait nucleotide (QTN) alleles in naturally occurring yeast (*Saccharomyces cerevisiae*) isolates have complex phenotypic effects depending on both genetic background and environmental context (Gerke *et al.* 2010). However, to make predictions about how a particular QTN may influence trait variation in a novel genetic (or environmental) context requires a more mechanistic understanding of how the QTN allele interacts with the genetic background to influence phenotypes, whether at the level of gene expression, cellular changes, morphology, behavior, etc. (Xu *et al.* 2013). This goal may involve mapping the background modifier loci to identify the genes and alleles responsible for the background dependence (*e.g.*, Chandler 2010; Duveau and Félix 2012), and testing which genes are misexpressed (and how severely) as a result of the mutation in different genetic backgrounds (*e.g.*, Dworkin *et al.* 2009). Only with such data will we be able to identify common patterns across traits, taxa, and mutations.

Accomplishing these goals will require tractable models. Such models should provide the ability to examine specific mutations across multiple wild-type backgrounds and genomic resources to facilitate the analysis of the modifiers. One such system is the fly (*Drosophila melanogaster*) wing. Several mutations affecting wing development have background-dependent phenotypic effects (Altenburg and Muller 1920; Nakashima-Tanaka 1967; Silber 1980; Dworkin and Gibson 2006; Debat *et al.* 2009), with selectable variation present in natural populations (Thompson 1975; Cavicchi *et al.* 1989). In one dramatic example, the *scalloped*^{E3} (*sd*^{E3}) mutation causes a moderately reduced, blade-like wing in the background of one common lab wild-type strain, Samarkand (hereafter, SAM), but a much more severely diminished wing in another common background, Oregon-R (ORE) (Figure 1; Dworkin *et al.* 2009). These two parental strains are commonly used wild-types for *Drosophila* research, one primarily in molecular biology (ORE), and the other (SAM) in quantitative genetics, aging, and studies of recombination (Hofmanova 1975; Hofmann *et al.* 1987; Lyman *et al.* 1996; Lyman and Mackay 1998; Leips and Mackay 2002; Mackenzie *et al.* 2011). More recently it was used as the common line for an advanced intercross design for the *Drosophila* synthetic population resource (King *et al.* 2012). Thus, identifying sequence polymorphisms and differences in gene expression between these two strains will facilitate studies of background dependence in other *Drosophila* traits.

The sets of genes whose expression is altered in wing imaginal discs by the *sd*^{E3} mutation in each genetic background are largely nonoverlapping and partially independent from those genes that are differentially expressed between the two genetic backgrounds in a wild-type context (Dworkin *et al.* 2009). The mechanisms underlying this background dependence, however, are poorly understood. Nevertheless, *sd* itself is well studied, making it a good system for investigating the mechanisms underlying background-dependent expression. SD encodes a TEA family transcription factor (TF) that forms heterodimers with multiple TF partners to regulate at least three biological processes (Campbell *et al.* 1992; Guss *et al.* 2013). Its best known role is in wing development, where SD interacts with the Vestigial (VG) protein (Halder *et al.* 1998; Paumard-Rigal *et al.* 1998; Simmonds *et al.* 1998; Bray 1999; Varadarajan and VijayRaghavan 1999; Guss *et al.* 2001; Halder and Carroll 2001). In particular SD-VG regulates the expression of a number of genes influencing specification of cell fates as well as overall tissue growth in the wing imaginal disc (Guss *et al.* 2001; Halder and Carroll 2001). Recently SD has been shown to be an important transcriptional cofactor with Yorkie (YKI), mediating hippo signaling to regulate growth and polarity of tissues (Goulev *et al.* 2008; Wu *et al.* 2008; Zhang *et al.* 2008, 2009; Zhao *et al.* 2008; Ren *et al.* 2010; Doggett *et al.* 2011; Nicolay *et al.* 2011; Zhang *et al.* 2011; Poon *et al.* 2012; Cagliero *et al.* 2013; Koontz *et al.* 2013; Sidor *et al.* 2013). Finally, SD plays a role in the development of odorant and gustatory neurons in the adult (Campbell *et al.* 1992; Shyamala and Chopra 1999; Ray *et al.* 2008), although the details of how it acts as a transcriptional regulator are less well known in this context.

Like other quantitative traits, the penetrance and expressivity of a mutation probably have a complex genetic basis. Indeed, in one high-throughput screen for conditionally essential genes in yeast, four or more modifier loci were necessary to explain the background dependence of numerous conditionally lethal gene deletions (Dowell *et al.* 2010). These background polymorphisms may also have multifactorial consequences, such as pleiotropic effects on other unrelated traits (Duveau and Félix 2012). In the case of our *Drosophila* wing model system, preliminary mapping efforts suggested the presence of a major-effect modifier on chromosome arm 2R near (but not in) *vg*. Yet the genetic background polymorphisms responsible for this background dependence remain unknown (Dworkin *et al.* 2009). Unfortunately, due to the typically complex genetic basis of background dependence, fine mapping these modifier loci to specific polymorphisms, or even genes, remains challenging (Zhang *et al.* 2013). However, we may be able to gain additional insight by integrating data from a variety of approaches. For instance, gene expression studies can identify genes whose expression is affected by a focal mutation in a background-dependent manner (Dworkin *et al.* 2009, 2011), providing a complementary set of candidate loci. Then, using whole-genome resequencing to search for polymorphic transcription factor binding sites (TFBSs) could help explain these background-dependent effects on gene expression.

The primary goal of this current study was to identify the genomic regions that contribute to the genetic background effects of *sd*^{E3}. To do so, we integrated data from a variety of

experimental sources to identify a robust set of candidate genes mediating the background dependence of the sd^{E3} mutation. These sources included: (i) replicated introgression lines to map the loci contributing to background dependence; (ii) whole-genome resequencing of the introgression and parental lines to predict polymorphic SD transcription factor binding sites; (iii) expression profiling from a digital gene expression experiment and two existing microarray experiments; and (iv) the results of a previously published screen for dominant modifiers of the sd^{E3} phenotype. Despite earlier work suggesting that there may be a single modifier of large effect (Dworkin *et al.* 2009), our mapping results indicate that this background dependence has a complex basis, encompassing several genomic regions each containing multiple candidate genes. Nevertheless, the additional data help narrow the list of candidates. In particular, patterns of allele-specific expression and SD binding site predictions suggest that *cis*-regulatory variants are not a major contributor to this background dependence. Finally, we extend recent results demonstrating that the majority of genetic interactions with sd^{E3} are background dependent (Chari and Dworkin 2013), to determine whether these are the result of quantitative non-complementation or higher-order genetic interactions. Our results demonstrate that the majority of tested background-dependent modifiers cannot be explained simply by variation at the locus interacting with *scalloped*, ruling out simple quantitative noncomplementation. Overall, our results lay the foundation for more detailed investigations into the mechanisms underlying genetic background dependence, and suggest that this approach should be useful for dissecting other complex phenotypes.

Materials and Methods

Mutations and wild-type strains

As described in detail in Dworkin *et al.* (2009), we introgressed the sd^{E3} allele into the SAM and ORE wild-type strains via backcrossing for >20 generations (each marked with w^- to facilitate the introgression). Each wild-type strain (both with and without the sd^{E3} mutation) was tested (using 8–10 molecular markers across the genome) to rule out contamination. Results from whole-genome resequencing (see below) were consistent with these initial results.

Generating short- and long-wing backcross lines for mapping

To map the loci underlying the background dependence of the sd^{E3} mutant phenotype, we used a phenotypic selection-based backcross procedure to introgress genomic regions that harbor the short-wing alleles into an otherwise long-wing genome (Figure 2). We generated a total of five independent backcross lines by crossing ORE *w* sd^{E3} flies to SAM *w* sd^{E3} flies, and crossing the F_1's together. From the F_2's, we selected flies with both long-wing (SAM-like) and short-wing (ORE-like) phenotypes. These flies were backcrossed to ORE *w* sd^{E3} and SAM *w* sd^{E3} flies, respectively, and the process was repeated. Twelve cycles of backcrossing (24 generations) were completed for the short-wing backcross lines, and 20 cycles (40 generations) for the long-wing lines, with 20 flies of each parent strain used for backcrossing each generation (Chari and Dworkin 2013). We generated four independent short-wing replicates. Only one long-wing replicate remained at the final generation, as maintaining the long-wing phenotype while backcrossing to ORE *w* sd^{E3} was problematic because inheritance patterns broke down over successive generations: specifically, the long-wing phenotype ceased being dominant (I. Dworkin, unpublished data).

Phenotyping of wing size

To compare wing lengths in the backcross lines, along with the "pure" SAM and ORE background sd^{E3} strains, we grew each of the lines at 24°, 65% relative humidity (RH) on a 12:12 light cycle in a Percival incubator (I41VLC8) using our standard lab media. Once flies eclosed, they were stored in 70% ethanol. Twenty wings were dissected from each genotype (10/sex) and mounted in 70% glycerol in PBS. Digital images were captured using an Olympus DP30BW camera mounted on an Olympus BW51 microscope at ×40 magnification. Wing area was then estimated using a custom ImageJ macro that segments the wing blade from the rest of the image.

Resequencing Oregon-R, Samarkand, and backcross lines

We prepared genomic DNA from frozen whole flies using a Zymo Research Tissue and Insect DNA kit (Irvine, CA) following the manufacturer's instructions and submitted samples to the Michigan State University Research Technology Support Facility for analysis on an Illumina Genome Analyzer II. SAM and ORE were each run on separate lanes while the five backcross lines were barcoded, pooled, and run on a single lane. We obtained ~30,000,000 paired-end 75-bp reads (with an estimated insert size of 360 bp) for each lane, yielding 24-29X coverage for SAM and ORE and 5-7X coverage for each of the backcross lines.

We mapped reads to the *D. melanogaster* reference genome (release 5.41) using bwa v. 0.6.0-r85 (Li and Durbin 2009), allowing up to four mismatches (5%) per read. We used samtools v. 0.1.18 (Li *et al.* 2009) to call SNPs in all samples simultaneously and to generate consensus sequences for ORE and SAM. Sites with coverage higher than 100 times were excluded from SNP calling to avoid false positives in repeat sequences. In downstream analyses of the backcross lines, we excluded indels and included only SNPs for which SAM and ORE were both scored as homozygous, but different from one another with high confidence (genotype quality scores ≥30 as reported by samtools).

Backcross analyses

For each backcross line, we sought to determine whether the genome at a particular genomic location was inherited from

SAM or ORE, so we focused our attention on SNPs at which SAM and ORE were scored as homozygous for different alleles. For each SNP, we estimated the frequency of the ORE (short wing) and SAM (long wing) alleles using custom Python scripts to count the number of sequence reads in each backcross line carrying each allele. We then plotted the proportion of reads displaying the ORE allele across the entire genome using a sliding window approach (with a window size of 10 kb and a step size of 2 kb). An alternate binning approach and various bin sizes yielded similar results.

SD binding site analyses

We sought to scan the ORE and SAM consensus genomes for genes that are predicted to be SD binding targets and in which sequence differences between SAM and ORE may alter putative SD binding sites. We first generated a position-weight matrix based on 23 known SD binding sites (Supporting Information, Table S1 and Table S2) using the MEME suite (Bailey *et al.* 2009). Next, for each annotated gene in the genome, we extracted its full sequence in ORE and SAM (including introns) plus 10 kb of upstream and downstream flanking sequence. We used MotifScan.v6 (Kim *et al.* 2010) to generate a log-likelihood ratio (LLR) score for each gene, indicating the relative likelihood that the sequence contains one or more SD binding sites. We computed the difference between the LLR scores obtained from the SAM and ORE consensus sequences (ΔLLR). To identify genes with the strongest evidence of having predicted SD binding sites in SAM or ORE, or of being background-dependent SD targets, we derived empirical *P*-values for the LLR and ΔLLR scores by comparing each gene's LLR and ΔLLR scores to the 1000 other genes with the most similar GC content.

To complement these genome-wide binding site analyses, we also investigated the sequences of two known SD binding sites that were previously experimentally verified, in the genes *cut* and *salm* (Guss *et al.* 2001; Halder and Carroll 2001), by extracting all sequence read data that mapped to those sites (using the mpileup command in samtools).

Digital gene expression

We used digital gene expression (Morrissy *et al.* 2009) to identify genes that are misregulated in sd^{E3} mutants and genes showing evidence of allelic imbalance in SAM/ORE "hybrids." This approach is similar to RNA-seq, but the cDNA is treated with a restriction enzyme (*Nla*III) during library preparation, causing all sequence reads to begin at a restriction site. We first generated both mutant and wild-type F_1 hybrids by crossing SAM *w* sd^{E3} flies to ORE *w* sd^{E3} flies. We dissected wing discs from wandering third instar larvae and pooled ~200 wing discs to generate each sample. We generated two biological replicates each of both wild-type and mutant hybrid flies. We extracted total RNA using an Ambion MagMax-96 kit (Life Technologies) following the manufacturer's instructions. Further processing was performed at the Michigan State University Research Technology Support Facility, where samples were sequenced on an Illumina Genome Analyzer. After quality filtering, we obtained 7.6 to 8.1 million single-end, 17-bp reads from each sample.

We appended the *Nla*III restriction site recognition sequence to the start of each sequence read and mapped sequence tags (unique reads) to the consensus ORE and SAM transcriptome sequences using BWA, allowing up to two mismatches (11%) per sequence. Sequences that mapped equally well to multiple genes were discarded from further analyses. All sequences that mapped to a single coding gene were included in analyses comparing wild-type flies to mutant flies. All sequence tags mapping to a single coding gene specifically in SAM or ORE were used in analyses of allelic imbalance. In cases in which either the SAM or ORE allele was missing from the sequence reads (*i.e.*, only one of the two alleles was transcribed), we examined the SAM and ORE genome sequences to check for mutations in the *Nla*III restriction sequence, because such a mutation would cause the mutation-bearing allele to be absent from our dataset even if it was being expressed. These cases were excluded from analyses of allelic imbalance.

To identify genes that are differentially regulated between wild-type and sd^{E3} mutant flies, we used the edgeR Bioconductor package for R v. 3.0.8 (Robinson *et al.* 2010), using the exactTest function, after estimating tagwise dispersions; all mapped reads were included in this analysis. We then computed *q*-values using the qvalue library (Storey and Tibshirani 2003). To test for allelic imbalance in genes in which sequence tags could be confidently assigned to either SAM or ORE, we compared binomial models using likelihood ratio tests. The null model assumed an equal probability (0.5) of a sequence read being derived from either SAM or ORE. The first alternative model allowed that probability to differ from 0.5, but was constrained to be the same in both wild-type and mutant flies. To identify genes in which the sd^{E3} mutation alters the level of allelic imbalance, we also tested a second alternative model, in which the probability that a given sequence read was derived from SAM or ORE differed between wild-type and mutant flies.

Microarrays

We compared the results of our digital gene expression (DGE) experiment to two similar microarray experiments: one using Drosophila Genome Research Center arrays (Dworkin *et al.* 2009), and one using a custom Illumina array (Dworkin *et al.* 2011). Raw array data are available at the National Center for Biotechnology Information Gene Expression Omnibus, NCBI GEO (GSE26706: GSM657471–GSM657487 and GSE13779: GSM346787–GSM346810). Briefly, genome-wide expression levels were quantified in wing discs of wandering third instar larvae with both wild-type and mutant (sd^{E3}) genotypes and both the SAM and ORE backgrounds. For each gene, we asked whether expression is influenced by genotype (wild type *vs.* sd^{E3}), genetic background (SAM *vs.* ORE), or an interaction between the two. For the Drosophila Genomics Resource Center (DGRC) dataset, we log transformed and normalized the data and fitted mixed models using the sample genotype, genetic

background, and their interaction as fixed effects, and array as a random effect, using the lmer function in R. For the Illumina dataset, we again log transformed and normalized the data, and fitted linear models (using the lm function), with genotype, background, and their interaction as predictor variables.

Modifier mapping

We examined results from a prior study that screened two large autosomal deletion libraries (Exelixis and DrosDel) for dominant, background-dependent modifiers of the sd^{E3} phenotype. Details are published elsewhere (Chari and Dworkin 2013). Briefly, we crossed males carrying each deletion to be tested to females carrying the sd^{E3} allele in either the SAM or ORE background. We analyzed the wing phenotypes of the male offspring, which were hemizygous for sd^{E3}, heterozygous for the deletion of interest, and heterozygous for one of the two backgrounds (Figure S4). As a control, we crossed SAM and ORE flies to the progenitor strains used to generate the deletion lines. We then scored wing phenotypes using a semiquantitative scale (1–10) (Chari and Dworkin 2013; Tanaka 1960), and used linear models to test for effects of each deletion, the genetic background, and their interaction on the wing phenotype. Deletions showing a significant interaction term were considered background-dependent modifiers. The raw data for the modifier mapping and for the subset of deletions used for the backcross selection can be obtained from the Dryad Digital Repository (http://dx.doi.org/10.5061/dryad.4dt7c).

Gene ontology analyses

Using the sets of candidate genes from the expression, deletion modifier screen, binding site analysis, and mapping data, we tested for overrepresentation of gene ontology categories using WebGestalt (Wang *et al.* 2013a) with the enrichment test tool. We performed analyses for individual datasets (using the appropriate reference gene list), as well as a combined analysis in which candidate genes were identified by searching for genes showing a congruent signal across multiple datasets (with the full Ensembl *Drosophila* gene list as the reference). We used a Benjamini–Hochberg false discovery rate, with a minimum of three genes per category. Given that for many genes we had only partial information (*e.g.*, for some genes we had no or incomplete expression data, while for genes on the X chromosome, we had no modifier data) this list is incomplete. However, it still provides a useful view of the types of genes represented and whether different subsets of biological processes are affected by the main genotypic effects of the sd^{E3} allele and by its interactions with other loci. We also verified our results using the BioProfiling.de tool (Antonov 2011), which is a superset of the analysis done by WebGestalt.

Results

Backcross mapping identifies genomic regions contributing to variation in the sd^{E3} phenotype

While the wings of the wild-type SAM and ORE flies are qualitatively similar, the effects of the sd^{E3} mutation differ dramatically in each background (Figure 1). To identify regions of the genome associated with the long- and short-wing sd^{E3} phenotypes, we backcrossed SAM or ORE sd^{E3} flies to the alternate background while selecting for short- and long-wing phenotypes, respectively, each generation (Figure 2). Backcrossing was repeated for 12 cycles (24 generations) for the short- and 20 cycles (40 generations) for the long-wing backcrosses. This procedure is expected to introgress the ORE alleles that contribute to a short-wing phenotype into an otherwise SAM background, and vice versa. After backcrossing, we obtained one long-wing and four short-wing lineages phenotypically similar to sd^{E3} in the pure SAM and ORE wild-type backgrounds (Figure 3), despite a predicted >95% replacement of the genetic background (Figure 4A).

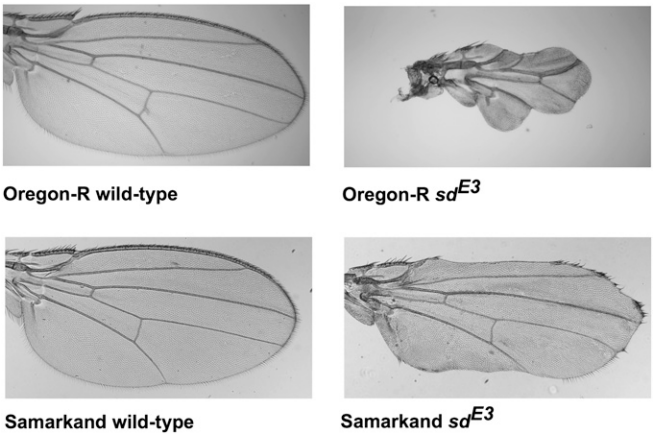

Figure 1 Phenotypic effects of the sd^{E3} mutation on the *Drosophila melanogaster* wing in the Oregon-R (ORE) and Samarkand (SAM) genetic backgrounds at ×40 magnification. While SAM and ORE wild-type wings are qualitatively similar, the phenotypic effects of the sd^{E3} are profoundly different across these two wild-type backgrounds.

To identify genomic regions harboring polymorphisms modulating genetic background effects, we used whole-genome resequencing of the parental and backcross strains to identify which genomic regions introgressed. While there were >504,000 putative polymorphisms identified between the ORE, SAM, and the reference genome, we utilized only 92,006 SNPs that met our criteria (see *Materials and Methods*). We observed several regions that introgressed repeatedly in the short-wing backcross lines, with sizes ranging from just a few kilobases, up to ~5 Mb (Figure 4B, Figure S1). A large portion of chromosome arm 3R introgressed, overlapping with several background-dependent modifier deletions of the sd^{E3} phenotype. There were several additional regions, all of smaller sizes, on chromosome arm 3L that also consistently introgressed. Nearly 75% of the left half of chromosome arm 2R introgressed in some backcross lines, and ~5 Mb of chromosome 2L also introgressed across all short backcross lines, although each with clearly distinct recombination breakpoints. Several regions were less consistent. For instance, while a portion of chromosome arm 2L introgressed repeatedly, the breakpoints around the introgressed region were variable among lines (Figure 4B, Figure S1), with one replicate line exhibiting

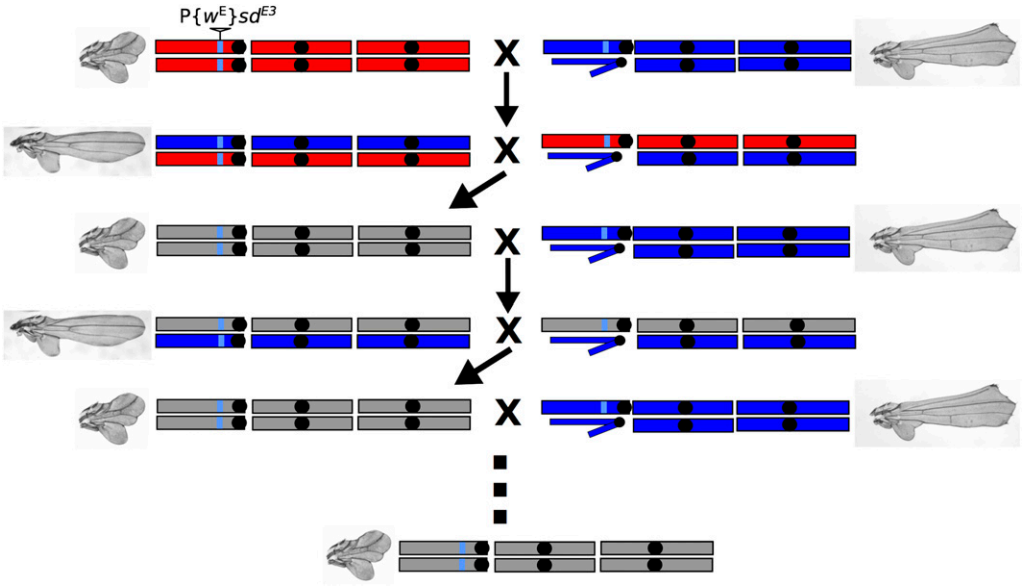

Figure 2 Backcross selection strategy used to introgress alleles from one background into another. The *sd*^{E3} allele (insertion denoted by gray triangle) was originally backcrossed into both the Samarkand background (blue) with the relatively less severe phenotype and Oregon-R (red) with higher expressivity (top row). The light blue genomic fragment proximal to the *sd*^{E3} allele represents the genomic region from the original genetic background that *sd*^{E3} was generated on (neither SAM nor ORE), while the gray coloration in generation three and beyond indicates unknown chromosomal composition due to recombination between the SAM and ORE chromosomes in previous generations. The two-generation cycle consisted of generating F_2's and selecting flies with the smallest wings and subsequently crossing these back to a pure SAM *sd*^{E3} background. This cycle was repeated 12 times and should theoretically replace ~95% of the genome, with the exception of the regions that contribute to the background-dependent variation for expressivity of the mutant phenotype.

nearly complete introgression of the entire chromosome arm.

In the long-wing backcross line, we expected the opposite genomic pattern from the short-wing lines, *i.e.*, mostly ORE alleles, except where long-wing SAM alleles had introgressed. We identified only a few regions exhibiting this pattern (Figure 4, Figure S1), some of which corresponded to the introgression regions for the short-wing backcross lines: one on the left half of chromosome arm 2L, one on the left half of 2R, one on 3L, and one on 3R. Surprisingly, in some regions where an ORE segment had introgressed into an otherwise SAM chromosome in the short-wing backcross lines, the same allelic distribution was observed in the long-wing backcross line, rather than the opposite pattern as expected for background modifiers of the *sd*^{E3} phenotype, *e.g.*, a small region near the right end of 3R (Figure 4, Figure S1).

Strain-specific polymorphisms in predicted SD binding sites weakly correlate to differences in gene expression

To identify putative polymorphic SD transcription factor binding sites that may contribute to the background-dependent effects of the *sd*^{E3} mutation on gene expression, we searched our resequenced SAM and ORE genomes with MotifScan v6 (Kim *et al.* 2010) for predicted SD targets. Using the LLR scores generated by MotifScan, we computed an empirical *P*-value for each gene by comparing its LLR score to the LLR scores of 1000 genes most similar in GC content (see *Materials and Methods* for details). A total of 163 genes were predicted to be targets of regulation by SD ($P \leq 0.01$ in either SAM or ORE; Table 1; see Dryad doi:10.5061/dryad.1375s for full results). Of these, 131 were common to both genetic backgrounds, 16 were SAM specific, and 16 were ORE specific. Genes predicted to be SD targets in at least one of the two backgrounds showed significant overlap with genes identified as being misexpressed in *sd*^{E3} flies in one of three gene expression datasets (the DGRC dataset; see *Integrating multiple datasets generates a robust set of candidate loci* below); however, the degree of overlap was not especially strong (using a more relaxed significance threshold to increase the total strength of the signal in the data, observed overlap = 16 genes of 10,380 common to both datasets, of which 146 were differentially expressed in DGRC at $q \leq 0.05$ and 535 were significant in the binding prediction analysis at $P \leq 0.05$; $P = 0.004$ in a randomization test).

In addition, we also searched for genes that showed evidence of differential affinity for SD between the SAM and ORE genomes by identifying genes with exceptional differences in LLR scores computed using the SAM and ORE sequences, regardless of whether or not the gene was predicted to be a significant SD target in our first analysis. Using this method, we identified 149 genes predicted to show differential affinity for SD ($P \leq 0.01$), although only 37 of these were predicted to be significant SD binding targets ($P \leq 0.01$).

We also manually checked two experimentally verified SD binding sites (Guss *et al.* 2001; Halder and Carroll 2001) for polymorphisms. The genes regulated by both of these binding sites were predicted to be SD binding targets by our analyses (*cut*: $P = 0.018$ in SAM and $P = 0.022$ in ORE; salm: $P = 0.026$ in SAM and $P = 0.023$ in ORE), but neither was predicted to show differential affinity for SD binding. There was no evidence of substitutions in the SD binding site that regulates *cut* expression (Table S3). However, ORE (but not SAM) showed evidence of three substitutions in the known SD binding site that regulates *salm* (Table S4). *salm* was one gene that was verified (via *in situ* hybridization) to be differentially expressed between SAM *sd*^{E3} and ORE *sd*^{E3} (Dworkin *et al.* 2009).

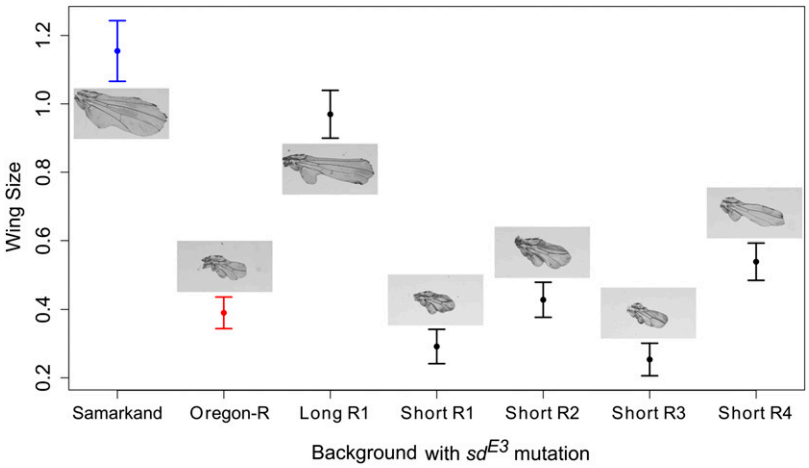

Figure 3 Comparison of wing phenotypes of parental (SAM and ORE) sd^{E3} flies, and of long- and short-wing backcross lines generated for this study, confirming phenotypic similarity between SAM and long-wing backcross lines, and between ORE and short-wing backcross lines.

Allelic imbalance in gene expression is unlikely to contribute to the phenotypic effects of genetic background

We generated DGE data—sequences from short mRNA tags (cleaved by a restriction enzyme)—in SAM/ORE hybrid flies with both wild-type (ORE sd^+/SAM sd^+) and sd^{E3} (ORE sd^{E3}/SAM sd^{E3}) genotypes. We used this to identify (i) genes that are misregulated in the presence of the sd^{E3} mutation; (ii) genes showing evidence of allelic imbalance, *i.e.*, unequal transcription of the SAM and ORE alleles of the same gene; and (iii) genes showing evidence of genotype-dependent allelic imbalance.

A total of 59,057 mappable unique sequence tags representing 11,267 transcripts from 10,312 genes were identified. Of these, 2,078 sequence tags representing 1,639 genes displayed significantly different expression levels between wild-type and sd^{E3} flies at a threshold of $q \leq 0.001$. This set of differentially expressed genes contained a disproportionate number of genes annotated as being involved in spindle organization and mitotic spindle organization, microtubule cytoskeleton organization, spindle elongation and mitotic spindle elongation, and gene expression, among others (Figure S2, Table S5).

Because DGE was performed in SAM/ORE hybrid flies, we also wanted to test for allelic imbalance, *i.e.*, differential expression of the two copies of a gene within an individual. There were 2583 mappable unique sequence tags representing 1970 transcripts and 1937 genes for which we could distinguish between the SAM and ORE alleles. Of those, 392 tags representing 378 genes showed evidence of allelic imbalance at a threshold of $q \leq 0.001$ (Table S6). Genes showing evidence of allelic imbalance were not enriched for any Gene Ontology (GO) categories after adjustment for multiple comparisons.

We identified 29 genes showing evidence of a difference in the level of allelic imbalance between wild-type flies and sd^{E3} mutant flies ($q \leq 0.001$; Table 2). There was no more overlap than expected by chance between these genes and genes showing evidence of differences in SD binding affinity between SAM and ORE ($P = 0.52$ using a randomization test, again with a more liberal significance cutoff; observed overlap = 11 genes of 1063 common to both datasets, of which 156 were significant in the DGE dataset at $P \leq 0.01$ and 71 were significant in the binding prediction dataset at $P \leq 0.05$). Similarly, these genes did not show any more overlap than expected by chance with the genes showing evidence of a genotype-by-background interaction influencing expression levels in either of two previously published microarray datasets ($P = 0.11$ and $P = 0.93$). Considering *sd* genotypes separately, 337 genes showed evidence of allelic imbalance in wild-type flies (at the same threshold), and 146 genes showed evidence of allelic imbalance in sd^{E3} flies, with 26 of these genes overlapping (all at $q \leq 0.001$). Again, GO terms showed no significant enrichment after correction for multiple comparisons. Lastly, there did not seem to be any overall, consistent bias toward the expression of one background's alleles or any consistent change in allelic imbalance between wild-type and mutant flies (Figure 5, Figure S3). Thus, despite some evidence of allelic imbalance, it does not appear to correlate well with other features of the background dependence. Whether this is a function of the underlying biology or the limited representation of the short sequence tags (limiting our ability to discern RNA from each parental allele) is unclear.

The majority of background-dependent genetic interactions with sd^{E3} cannot be explained by quantitative noncomplementation across the wild-type strains

A previous deletion screen for dominant modifiers of the sd^{E3} phenotype showed that the majority of observed modifiers display background dependence (Chari and Dworkin 2013). That is, most deletions that alter the sd^{E3} phenotype do so differently when expressed in the SAM and ORE genetic backgrounds. However, that study was unable to distinguish between two competing hypotheses to explain this result. The first is quantitative noncomplementation, *i.e.*, second-order epistasis between the sd^{E3} allele and the hemizygous background allele uncovered by the deletion (Palsson and Gibson 2000; Mackay *et al.* 2005). Alternatively, background-dependent modifiers may be explained by third-order (or higher) epistasis between the sd^{E3} allele, the deletion itself, and one or more

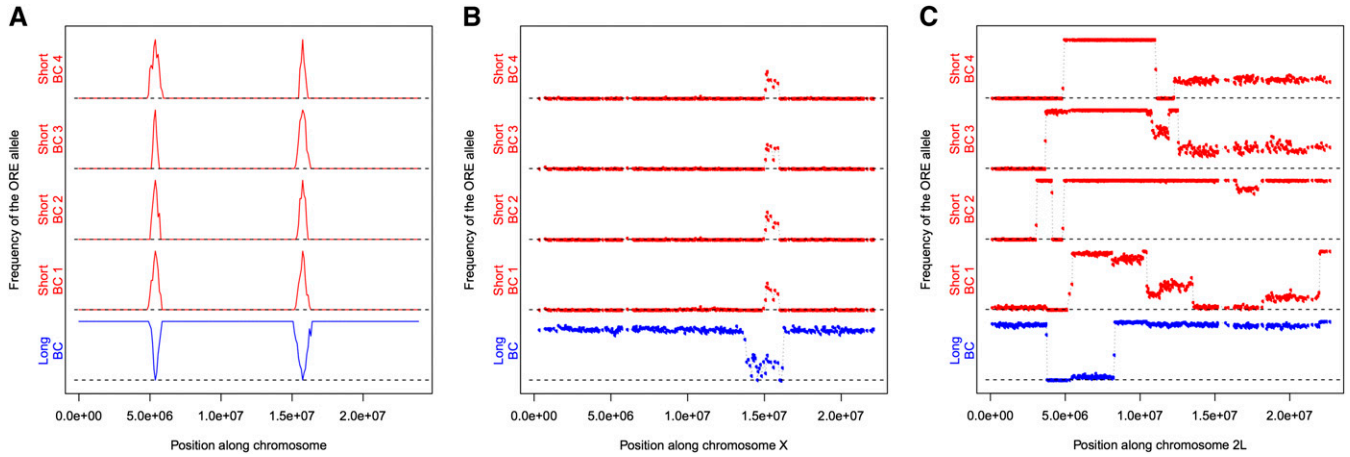

Figure 4 Introgression of genomic fragments among the selection-backcross lineages. (A) Idealized expectations for the frequency of the ORE allele along the length of a chromosome arm in short- and long-wing sd^{E3} backcross lines; spikes in allele frequencies should indicate loci contributing to the background-dependent wing phenotype differences. (B and C) Observed frequency of the ORE allele along the length of chromosome arms X and 2L in short- and long-wing sd^{E3} backcross lines. In B, the peak corresponds to the position of the introgression of the sd^{E3} mutation, and thus represents a good positive control that the method is working. Allele frequency spikes are expected around *sd* because the sd^{E3} allele was originally introgressed into SAM and ORE from another genetic background, and therefore the surrounding region still carries the haplotype of the sd^{E3} progenitor strain, containing a mixture of SNPs that distinguish SAM and ORE. In C, variation in the extent of the introgressed fragment (with independent breakpoints) is observed.

genetic background alleles elsewhere in the genome. To evaluate these hypotheses, we used data from crosses between 31 deletions showing background-dependent effects to the short- and long-wing introgression lines (Figure 2, Figure S4). If the modifier deletion's background dependence is due to quantitative noncomplementation, then the wing phenotype will depend on the genetic background (SAM or ORE) the fly carries across from the deletion. On the other hand, if this background dependence is due to higher-order epistasis, the phenotype will also depend on alleles present at other locations in the genome, not just alleles uncovered by the deletion.

We can therefore test for quantitative noncomplementation by comparing the genotypes and phenotypes of flies carrying a deletion of interest and the sd^{E3} mutation in (i) a pure SAM or ORE parental background, *vs.* (ii) an introgression background. Specifically, if flies from these two cases exhibit the same modification of the wing phenotype, but are hemizygous for different alleles at the deletion locus, then alleles elsewhere in the genome must be influencing how the deletion modifies sd^{E3}'s effects, and we can rule out a "simple" two-way interaction (Figure S4). Similar logic applies for the situation in which the lineages have distinct phenotypes but the same allele opposite the deletion. For ~80% of the deletions tested, at least one cross between a backcross and the deletion provided evidence that second-order epistasis is insufficient to explain the background dependence of the modifier's effects (Table 3). Thus, the majority of modifier loci are background dependent because of third- or higher-order epistasis between the focal mutation, the modifier, and additional loci elsewhere in the genome.

Integrating multiple datasets generates a robust set of candidate loci

We also took advantage of several additional datasets. First, we used two previously published microarray datasets comparing gene expression profiles between wild-type and sd^{E3} flies in both the SAM and ORE genetic backgrounds to identify genes whose expression levels are influenced by *sd* genotype, genetic background, and their interaction (Dworkin *et al.* 2009, 2011). Second, we examined the results of the screen for autosomal dominant modifiers of sd^{E3} mentioned earlier (Chari and Dworkin 2013).

To identify candidate genes for further study, we searched for genes displaying a common signal in multiple datasets: (i) those falling within a region showing evidence of introgression in the short-wing backcross lines; (ii) genes occurring within modifier deletions or background-dependent modifier deletions; (iii) differentially expressed genes in the microarray and DGE datasets (specifically, genes whose transcript levels were influenced by *sd* genotype, a genotype-by-background interaction in the microarray datasets, or genotype-dependent allelic imbalance in the DGE dataset); (iv) genes predicted to show differential affinity for SD binding between SAM and ORE. Because significant but incongruent effects in independent expression datasets (*e.g.*, up-regulation in sd^{E3} flies in one dataset, and down-regulation in another dataset) could be a cause for concern, we also "flagged" genes showing evidence of such inconsistency. We then plotted all of these sources of data on a common set of axes (Figure 6, Figure S5) and selected a set of robust candidates supported by multiple independent data types, including multiple expression datasets. At this stage, we used liberal cutoffs to identify "significant" genes ($q < 0.05$ for most datasets; $P < 0.05$ for SD binding and the Illumina microarray dataset; and short-wing allele frequency ≥ 0.6 for the mapping-by-introgression dataset), because we were interested only in those genes showing a consistent signal across multiple datasets.

Table 1 Top 50 genes predicted to be targets of regulation by SD in the SAM and ORE genetic backgrounds

Gene	P_{SAM}	P_{ORE}	P_{Diff}
nej	0.001	0.003	0.423
CG3795	0.001	0.001	0.043
5SrRNA-Psi:CR33371	0.001	0.001	0.39
Uch-L5R	0.001	0.004	0.001
cdi	0.002	0.001	0.001
5SrRNA:CR33434	0.001	0.001	0.048
CG14752	0.005	0.001	0.007
Apf	0.002	0.001	0.013
Muc14A	0.001	0.001	0.001
Muc12Ea	0.001	0.001	0.001
na	0.001	0.004	0.001
Cht6	0.001	0.001	0.038
PGRP-LB	0.001	0.001	0.031
CR43211	0.001	0.001	0.008
CG6084	0.002	0.006	0.148
Myo10A	0.003	0.002	0.103
5SrRNA:CR33370	0.002	0.002	0.11
5SrRNA:CR33377	0.002	0.002	0.072
CG32669	0.002	0.003	0.155
CG11180	0.002	0.002	0.03
feo	0.002	0.002	0.05
Hexo2	0.002	0.003	0.09
5SrRNA:CR33433	0.002	0.002	0.091
5SrRNA:CR33445	0.002	0.002	0.156
5SrRNA:CR33447	0.002	0.002	0.135
Trxr-1	0.002	0.003	0.009
rtv	0.005	0.002	0.002
ND75	0.002	0.002	0.006
Reg-2	0.007	0.002	0.005
CG42832	0.002	0.002	0.002
CG31907	0.004	0.002	0.009
CG16742	0.002	0.003	0.163
CG17287	0.002	0.005	0.116
Rcd6	0.004	0.002	0.017
Rab9Fb	0.004	0.002	0.06
CG13917	0.004	0.002	0.032
CG7530	0.007	0.003	0.001
CG14551	0.003	0.004	0.001
snoRNA:Me18S-G962	0.008	0.003	0.001
Bx	0.011	0.003	0.002
Trx-2	0.013	0.003	0.002
sofe	0.003	0.004	0.036
ush	0.004	0.003	0.019
5SrRNA:CR33372	0.003	0.003	0.132
5SrRNA:CR33448	0.003	0.003	0.137
5SrRNA:CR33435	0.003	0.003	0.041
5SrRNA:CR33450	0.003	0.004	0.19
CG17290	0.008	0.003	0.004
CG6481	0.003	0.005	0.073
CG13056	0.003	0.006	0.045

P_{SAM}, P_{ORE}: *P*-value for being a predicted SD-binding target in SAM and ORE, respectively. P_{diff}: *P*-value for differential SD binding affinity between the SAM and ORE backgrounds.

By integrating all these results, we generated a set of "high confidence" candidates (Table 4) that mediate or are modulated by either the effect of genotype (sd^{E3} *vs.* wild type) or an interaction between genotype and wild-type genetic background. Not surprisingly, some well-known genes that interact with or are regulated by SD, such as *vg*, *bi/Omb*, *fj*, *Dll*, and *chico*, are found among these candidates. More generally we observed overrepresentation of genes involved with *Drosophila* wing development (Figure S6) for both the main and background-dependent interaction effects. There was also modest enrichment of microtubule-associated genes for genotypic effects, and RAS GTPases and intracellular membrane-bounded organelle genes for the interaction effects, although it is currently unclear whether these distinctions reflect a true difference among the types of gene products that mediate background dependence.

Discussion

The genomic context in which an allele finds itself can profoundly influence that allele's phenotypic consequences. Here, we have integrated genomic data from multiple experiments to examine how that context modulates the phenotypic effects of a specific mutation, the $scalloped^{E3}$ allele, on the *D. melanogaster* wing. Although these datasets did not always yield a congruent signal, we were able to identify several strong candidate regions likely to be involved in mediating the background dependence of this allele's effects on wing development. Importantly, each dataset in isolation yielded a large set of candidates; only by examining these disparate sources together were we able to identify a robust and practical set of candidates for more focused study.

Mapping by introgression

Using introgression to map the polymorphisms responsible for modulating sd^{E3}'s consequences on wing phenotypes points to a complex genetic basis for this background dependence. However, pinning this background dependence on specific polymorphisms or even specific regions is complicated by several difficulties. First, large chromosomal blocks introgressed in many cases, each containing many genes. One possible explanation for this result is selection for multiple linked alleles, which would drag the entire segment to fixation, essentially building a long large-effect quantitative trait locus out of many smaller ones. In this case, additional crosses to generate recombination events within these regions may prove fruitful in pinpointing the polymorphisms responsible for sd^{E3}'s background-dependent effects.

An alternative, but not necessarily mutually exclusive, explanation is that the causal polymorphisms lie within polymorphic inversions, suppressing recombination within these blocks. A related and intriguing hypothesis is that rearrangements themselves may be responsible for the background dependence, making it not only impossible but also illogical to map the background modifiers to individual SNPs. By looking for sequence read pairs that mapped to discordant genomic positions, we found little evidence that inversions relative to the reference *D. melanogaster* genome are present in these regions, as each putative inversion is supported by only a few discordant read pairs, there are multiple conflicting inversions within each strain, and few putative inversions appear polymorphic between SAM and ORE (Figure S7). We

Table 2 Genes showing evidence of genotype-dependent allelic imbalance in SAM/ORE "hybrid" wild-type and sd^{E3} mutant flies

Gene	ORE count (mut. 1)	SAM count (mut. 1)	ORE count (mut. 2)	SAM count (mut. 2)	ORE count (WT 1)	SAM count (WT 1)	ORE count (WT 2)	SAM count (WT 2)	*P*	*q*
CG6308	0	115	0	109	96	0	0	0	5.13E-87	6.50E-84
Reg-2	92	2	69	5	33	36	52	34	7.51E-20	4.76E-17
CG12708	2	117	0	0	38	31	0	0	5.17E-19	2.18E-16
CG3632	1	41	0	55	26	31	30	28	2.39E-18	7.57E-16
CG6739	7	1	9	2	0	17	0	21	8.79E-13	2.23E-10
mthl10	8	0	9	0	0	5	0	6	9.05E-10	1.91E-07
mtm	9	0	5	0	0	7	0	5	2.09E-09	3.78E-07
CG4452	14	8	5	12	22	0	17	0	3.72E-09	5.89E-07
CG33785	2	5	5	7	19	0	15	0	1.81E-08	2.52E-06
CG6310	75	82	85	75	50	102	30	102	1.99E-08	2.52E-06
CG2147	13	0	19	0	26	0	0	25	2.73E-08	3.14E-06
CG9281	0	14	0	17	7	9	8	3	6.49E-08	6.85E-06
CG1908	16	3	16	4	4	27	11	12	9.89E-08	9.64E-06
Spt5	93	45	74	55	81	105	73	111	1.66E-07	1.45E-05
mth	65	13	0	0	49	57	63	51	1.72E-07	1.45E-05
CG1140	30	6	21	5	8	13	10	20	2.16E-07	1.71E-05
CG1542	10	14	14	15	33	3	22	4	3.03E-07	2.26E-05
CG6051	15	2	8	3	5	25	11	17	1.03E-06	6.89E-05
U3-55K	0	0	32	62	42	22	34	14	1.03E-06	6.89E-05
CG5704	4	0	2	0	0	7	0	6	1.13E-06	7.14E-05
CG32202	1	8	0	9	12	1	11	9	2.31E-06	1.39E-04
CG5626	1	19	1	18	9	12	11	8	2.42E-06	1.39E-04
CG16888	0	2	0	3	7	0	7	0	2.87E-06	1.58E-04
scaf6	0	3	0	3	3	0	7	0	4.20E-06	2.22E-04
CG16799	0	18	0	12	7	8	5	9	6.75E-06	3.42E-04
RpL7-like	0	0	345	239	0	0	279	325	8.50E-06	4.14E-04
CAH2	4	10	0	0	13	0	8	1	1.04E-05	4.90E-04
CG4908	21	6	15	10	5	19	6	13	1.62E-05	7.33E-04
CG1673	0	2	0	5	2	0	4	0	2.27E-05	9.94E-04
CG2260	0	0	120	34	122	69	106	88	2.63E-05	1.09E-03
Chc	4	0	7	0	10	13	2	8	2.66E-05	1.09E-03
RpL7-like	5	1	5	3	0	7	2	16	2.94E-05	1.16E-03
CG30286	0	6	0	5	2	0	2	0	3.03E-05	1.16E-03
CG9005	0	3	0	5	0	0	5	0	3.15E-05	1.17E-03
Pep	1	3	3	8	10	0	0	0	3.94E-05	1.43E-03
CG12424	3	0	5	1	2	22	5	10	4.53E-05	1.51E-03
Khc-73	2	0	4	0	0	3	0	3	4.53E-05	1.51E-03
CG13749	0	3	0	3	4	0	2	0	4.53E-05	1.51E-03
CG12009	2	2	2	4	8	0	12	0	4.70E-05	1.53E-03
D12	15	5	0	0	5	19	5	16	5.00E-05	1.56E-03
Aats-glupro	8	1	4	0	1	3	1	7	5.04E-05	1.56E-03
CG5144	3	0	2	0	0	2	0	5	5.40E-05	1.62E-03
Lap1	3	4	10	4	34	2	30	0	5.59E-05	1.62E-03
CG17841	24	4	17	3	15	19	21	16	5.61E-05	1.62E-03
Eip71CD	0	0	9	0	0	0	0	4	6.17E-05	1.70E-03
CG7376	0	0	0	4	5	0	4	0	6.17E-05	1.70E-03
CG10650	4	1	4	0	0	5	0	2	6.67E-05	1.70E-03
CG15382	1	1	6	0	0	5	0	3	6.67E-05	1.70E-03
Not1	4	1	3	0	0	6	0	2	6.67E-05	1.70E-03
CG5189	6	1	6	0	0	1	0	4	6.81E-05	1.70E-03

P-values are derived from likelihood ratio tests comparing a model with genotype-dependent allelic imbalance to a model with the same level of allelic imbalance in wild-type and sd^{E3} flies, and *q*-values were generated using the qvalue package in R. Top 50 genes are shown.

therefore think this hypothesis is unlikely to explain the large introgression blocks.

In a few instances, the same allele became fixed in both short- and long-winged backcross lines, even though alternate alleles were expected to be selected in these contrasting treatments. These loci may have been influenced by unintended selection for alleles influencing viability, rather than for wing phenotypes. Indeed, such unanticipated genetic effects have been observed in other studies (*e.g.*, Seidel *et al.* 2008; Ross *et al.* 2011; King *et al.* 2012). Moreover, there was some inconsistency among introgression lines. We therefore propose that studies intending to map trait variation using an introgression-and-resequencing approach (*e.g.*, Earley and Jones 2011) must include reciprocal crosses and multiple replicates. A single replicate of this introgression in only a single direction, for instance, would have missed some introgression

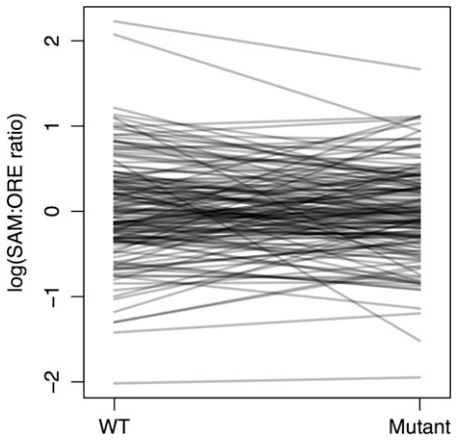

Figure 5 Allelic imbalance does not show a general pattern of perturbation in the sd^{E3} mutants. Allelic imbalance in SAM/ORE "hybrid" flies with both wild-type and sd^{E3} genotypes. Only sequence tags represented by at least five reads of each allele in all samples are represented in this plot.

regions, and some of the identified regions of introgression may have more to do with viability than with the trait of interest.

It is clear that multiple loci are involved, and problems generating multiple replicates of the long-winged backcross line (not shown) may indicate complex epistatic interactions between these loci. Although widely used with great success for Mendelian traits, the mapping-by-introgression approach adopted in the first part of our study may not be well suited to mapping trait variation with such a complex genetic basis. Nevertheless, in conjunction with the results of additional experiments such as gene expression data, this approach can still provide useful information that helps identify candidate genes for further investigation.

Majority of background-dependent modifiers cannot be explained by quantitative noncomplementation

An earlier study showed that the majority of the sd^{E3} allele's modifiers have effects that are background dependent (Chari and Dworkin 2013). Here, we extend that finding by providing evidence that these modifiers' background dependence is, in most cases, due to higher-order epistasis—interactions between the focal mutation (in this case, sd^{E3}), the modifier itself (in this case, a deletion), and alleles elsewhere in the genome. This finding is consistent with growing evidence that higher-order epistasis is prevalent (Weinreich *et al.* 2013) and that what may initially seem to be a two-way interaction is often a more complex interaction involving additional loci or environmental influences (Whitlock and Bourguet 2000; Gerke *et al.* 2010; Wang *et al.* 2013b; Lalić and Elena 2013). To our knowledge this is the first attempt at combining such genetic and genomic data to infer the order of epistatic interactions (or at least to rule out lower-order interactions). While this approach can only be used for genetically and genomically tractable systems, it does allow for making a clear inference even in the absence of the exact identity of some of the interacting partners. Prior results are consistent with the hypothesis that the background loci altering interactions between sd^{E3} and its modifiers are the same as those mediating the background dependence of sd^{E3} itself (Chari and Dworkin 2013). Thus, identifying the latter should provide insights into the former, and further experiments can shed light on the precise nature of these interactions.

Binding site analyses

Using the whole-genome sequence data for SAM and ORE, we identified a large number of predicted SD binding sites. More relevant for this study, we also identified a moderate number of genes whose regulatory elements are predicted to bind SD differentially between the SAM and ORE genetic backgrounds. Nearly all of these await experimental validation. In addition, binding predictions were only weakly correlated with expression differences. This result should not be too surprising, as the set of genes whose expression changes in the presence of the sd^{E3} mutation includes both direct and indirect targets of SD. Nevertheless, two validated targets of SD binding were picked by our approach as predicted targets of SD regulation. While one of these was manually found to contain three polymorphisms in the SD binding site, this differential SD binding affinity was missed by our analysis. Moreover, while exploring different binding site prediction methods, we also found that results were highly dependent upon the approach used as well as on the choice of specific position weight matrix (not shown).

Combined, these observations suggest that current binding site prediction approaches may not be specific or sensitive enough to produce completely reliable sets of candidate regulation targets on their own. Even so, they still seem to possess enough predictive power that, when combined with other sources of data, they can strengthen the evidence for the involvement of some genes in a biological process of interest. For instance, several of the candidate genes that were already strongly supported by other sources of data were also predicted to be SD binding targets or to possess polymorphic SD binding sites (Table 4).

Gene expression

Though the direction of effects was mostly consistent, the same genes were not always identified as significant in independent expression datasets. These differences may be explained by the unique technologies used with different biases, as well as distinct experimental designs. For example, the DGE experiment could only measure the abundance of transcripts containing the restriction sequence (CATG), may have been subject to biases in mapping reads to the reference genome, and our ability to detect background-dependent expression was contingent on the presence of SNPs in our sequence reads derived from SAM-ORE hybrid flies. The microarray datasets, on the other hand, used only flies with either a pure SAM or ORE background, and each array could only measure the expression of the specific transcripts complementary to the arrays' probes, which may

Table 3 Results of tests to distinguish between second- and higher-order epistasis to account for background-dependent dominant modifiers of the *sd^{E3}* phenotype

Deletion	Deletion name	Chr	Start	End	S1.SAM	S1.ORE	S3.SAM	S3.ORE	L1.SAM	L1.ORE
6326	Control	NA	NA	NA	−2.75 to −2.39, ORE	−0.11 to 0.21, ORE	−2.69 to −2.3, ORE	−0.21 to 0.16, ORE	−0.47 to 0.07, SAM	2.06 to 2.58, SAM
7491	Df(2L)Exel6004	2L	1,074,079	1,158,137	−1.81 to −0.37, SAM*	−0.82 to 0, SAM*	−2.23 to −0.34, SAM*	−0.79 to 0.36, SAM*	−1.48 to 0.63, ORE*	0.31 to 1.84, ORE*
7492	Df(2L)Exel6005	2L	1,555,098	1,737,249	−3.14 to −2.57, SAM*	0.69 to 2.36, SAM	−3.65 to −2.92, SAM*	1.08 to 2.82, SAM	−0.43 to 0.14, ORE*	0.36 to 2.03, ORE*
7503	Df(2L)Exel6017	2L	7,202,317	7,418,128	−1.72 to −0.95, ORE	0.63 to 1.14, ORE*	−1.49 to −0.32, ORE	0.03 to 0.89, ORE	−0.49 to 0.68, SAM	0.11 to 0.97, SAM
7505	Df(2L)Exel6021	2L	8,989,308	9,176,164	−1.6 to −0.33, Ambig	−0.35 to 1.11, Ambig	−1.12 to −0.18, ORE	−0.47 to 0.6, ORE	−0.56 to 0.39, ORE*	−0.04 to 1.04, ORE
7516	Df(2L)Exel6033	2L	12,423,459	12,655,793	−1.03 to −0.04, Ambig	−0.79 to 0.36, Ambig	−1.87 to −0.3, Ambig	−0.59 to 1.25, Ambig	−0.44 to 0.61, ORE*	0.22 to 1.45, ORE*
7524	Df(2L)Exel6042	2L	18,973,942	19,161,727	−3.14 to −1.14, Ambig	−1.38 to 0.81, Ambig	−2.69 to −1.06, Ambig	−1.49 to 0.38, Ambig	NA	1.83 to 3.02, ORE*
7525	Df(2L)Exel6043	2L	19,161,727	19,423,709	−2.58 to −0.97, Ambig	−1.3 to 0.85, Ambig	−3.02 to −1.26, Ambig	−1.06 to 1.35, Ambig	−0.91 to 0.34, ORE*	0.68 to 2.74, ORE*
7529	Df(2L)Exel6047	2L	21,102,742	21,244,119	−2.67 to −1.38, Ambig	−0.65 to 1.7, Ambig	−2.97 to −1.14, Ambig	−0.69 to 1.8, Ambig	−0.47 to 0.14, ORE*	0.31 to 2.36, ORE*
7540	Df(2R)Exel6058	2R	4,215,033	4,332,249	−2.61 to −1.71, ORE	−1.26 to 0.2, ORE	−2.77 to −1.84, ORE	−1.13 to 0.35, ORE	−0.81 to 0.06, Ambig	1.48 to 3.15, Ambig
7541	Df(2R)Exel6059	2R	6,761,890	7,073,552	−1.22 to −0.27, Ambig	−0.14 to 0.5, Ambig	−0.99 to 0.07, Ambig	−0.43 to 0.22, Ambig	−0.27 to 0.63, Ambig	0.41 to 1.08, Ambig
7544	Df(2R)Exel6062	2R	8,868,689	8,922,684	−2.71 to −1.58, Ambig	−1 to 0.74, Ambig	−2.47 to −1.84, Ambig	−0.72 to 0.48, Ambig	−1.34 to −0.09, SAM*	0.67 to 2.45, SAM
7554	Df(2R)Exel6072	2R	16,944,303	17,138,350	−2.95 to −2.05, SAM*	−1.07 to 0.57, SAM*	−3.05 to −2.2, SAM*	−0.85 to 0.6, SAM*	−1.5 to 0.36, SAM	1.13 to 3.22, SAM
7585	Df(3L)Exel6106	3L	5,601,375	5,684,102	−1.18 to −0.38, Ambig	NA	−1.14 to −0.41, SAM*	0 to 0, SAM*	−0.56 to 0.33, ORE*	0.29 to 1.05, ORE*
7611	Df(3L)Exel6132	3L	17,414,682	17,526,127	−2.24 to −0.74, Ambig	−0.17 to 0.95, Ambig	−2.24 to −0.74, ORE	−0.17 to 0.95, ORE	−1.08 to 0.91, Ambig	0.17 to 1.86, Ambig
7625	Df(3R)Exel6146	3R	2,988,409	3,317,319	−2.36 to 0.67, Ambig	−1.59 to 1.73, Ambig	−2.85 to −0.69, ORE	−0.4 to 2.4, ORE	−0.43 to 2.03, Ambig	−0.19 to 3.33, Ambig
7677	Df(3R)Exel6198	3R	19,967,091	20,096,927	−2.07 to −0.96, Ambig	−1.18 to -0.06, Ambig	−3.06 to −1.88, SAM*	−0.26 to 0.93, SAM*	−0.13 to 0.53, ORE*	1.95 to 2.72, ORE*
7686	Df(3R)Exel6208	3R	22,983,208	23,079,244	−0.78 to 0.05, SAM	−0.28 to 0.34, SAM*	−0.49 to 0.04, SAM	−0.32 to 0.08, SAM*	−0.47 to 0.03, SAM	−0.08 to 0.31, SAM*
7724	Df(2L)Exel6256	2L	5,555,049	5,658,629	−3.06 to −2.29, ORE	−0.34 to 0.39, ORE	−3.3 to −2.34, ORE	−0.3 to 0.63, ORE	−0.19 to 0.84, SAM	2.49 to 3.47, SAM
7741	Df(3R)Exel6274	3R	19,001,169	19,121,356	−2.33 to −0.67, SAM*	−1.2 to 0.78, SAM*	−2.91 to −1.66, SAM*	−0.45 to 1.59, SAM*	−0.45 to 0.17, ORE*	0.68 to 2.46, ORE*
7795	Df(2L)Exel7021	2L	4,915,628	4,979,299	−3.26 to −0.94, SAM*	−0.14 to 0.47, SAM*	−3.3 to −1.3, ORE	−0.06 to 0.8, ORE	−1.28 to 2.41, SAM	1.85 to 3.15, SAM
7834	Df(2L)Exel7067	2L	16,728,375	16,824,908	−2.86 to −1.71, SAM*	−1.14 to 1.99, SAM*	−3.51 to −1.97, Ambig	−0.49 to 2.26, Ambig	−2.41 to −0.16, ORE	−1.19 to 2.33, ORE
7845	Df(2L)Exel7073	2L	18,859,186	19,022,139	−2.63 to −1.66, Ambig	−1.1 to 0.31, Ambig	−2.93 to −2.21, Ambig	−0.55 to 0.62, Ambig	−0.26 to 0.26, ORE*	2.03 to 3.04, ORE*
7875	Df(2R)Exel7130	2R	9,960,585	10,100,288	−2.47 to −1.69, Ambig	−0.91 to 0.66, Ambig	−3.13 to −2.28, Ambig	−0.36 to 1.37, Ambig	0.03 to 0.65, SAM*	1.97 to 3.12, SAM
7879	Df(2R)Exel7135	2R	11,017,461	11,150,447	−1.49 to −0.22, ORE	NA	−1.6 to −0.12, Ambig	0 to 0, Ambig	−1.06 to 0.47, SAM	−0.06 to 1.19, SAM*
7894	Df(2L)BSC50	2R	14,509,027	14,618,276	−3.25 to −2.51, ORE	0.08 to 1.07, ORE*	−3.38 to −2.39, SAM*	−0.09 to 1.23, SAM*	−0.39 to 0.38, ORE*	1.81 to 2.8, ORE*
7949	Df(3L)Exel9065	3L	21,510,121	21,516,264	−0.76 to −0.04, Ambig	−0.35 to 0.35, Ambig	−1.19 to −0.22, ORE	−0.11 to 0.72, ORE	−0.37 to 0.14, ORE*	−0.07 to 0.64, ORE
7960	Df(3R)Exel7309	3R	7,472,850	7,541,866	−1.27 to 1.56, Ambig	−1.98 to 1.98, Ambig	−1.81 to −0.48, ORE	−0.39 to 2.97, ORE	−0.49 to 2.15, Ambig	−1.35 to 2.73, Ambig
7976	Df(3R)Exel8159	3R	9,809,236	10,085,649	−1.06 to −0.5, Ambig	NA	−1.04 to −0.51, ORE	0 to 0, ORE	−0.97 to 0.27, ORE*	−0.22 to 1.08, ORE
7993	Df(3R)Exel8178	3R	20,096,927	20,353,553	−2.83 to −1.43, Ambig	0.12 to 1.33, Ambig	−3.85 to −2.05, SAM*	0.7 to 2.4, SAM	−2.48 to −0.25, ORE	−0.92 to 0.99, ORE
7995	Df(3R)Exel9025	3R	25,570,975	25,585,907	−3.01 to −0.56, SAM*	0 to 2.23, SAM*	−0.96 to −0.38, SAM*	0 to 0, SAM*	−0.82 to 0.35, ORE*	0.02 to 0.83, ORE
7998	Df(2L)BSC50	2R	16,758,362	16,887,668	−3.08 to −2.42, SAM*	−0.4 to 0.57, SAM*	−4.15 to −2.3, SAM*	−0.41 to 1.52, SAM*	−3.39 to −1.71, SAM*	−0.85 to 1.08, SAM*

Short- and long-backcross strains were crossed to deletion mutants, and wing phenotypes were compared to those of offspring from crosses between the deletion and the parental SAM *sd^{E3}* or ORE *sd^{E3}* strains. Deletion, deletion name, Chr, start, and end provide the identities and chromosomal locations of the deletions tested. Remaining columns indicate results of pairwise comparisons between backcross × deletion flies (S1, short backcross 1; S3, short backcross 3; L1, long backcross) and the parental × deletion flies (SAM or ORE). Numbers indicate 95% confidence intervals for mean differences in wing phenotypes in each comparison, and "ORE," "SAM," and "Ambig" inside each cell indicates the hemizygous allele carried by that backcross strain at the deletion locus. Asterisks indicate comparisons in which the results rule out second-order epistasis (*i.e.*, flies have indistinguishable wing phenotypes but different alleles opposite the deletion, or different phenotypes but the same allele).

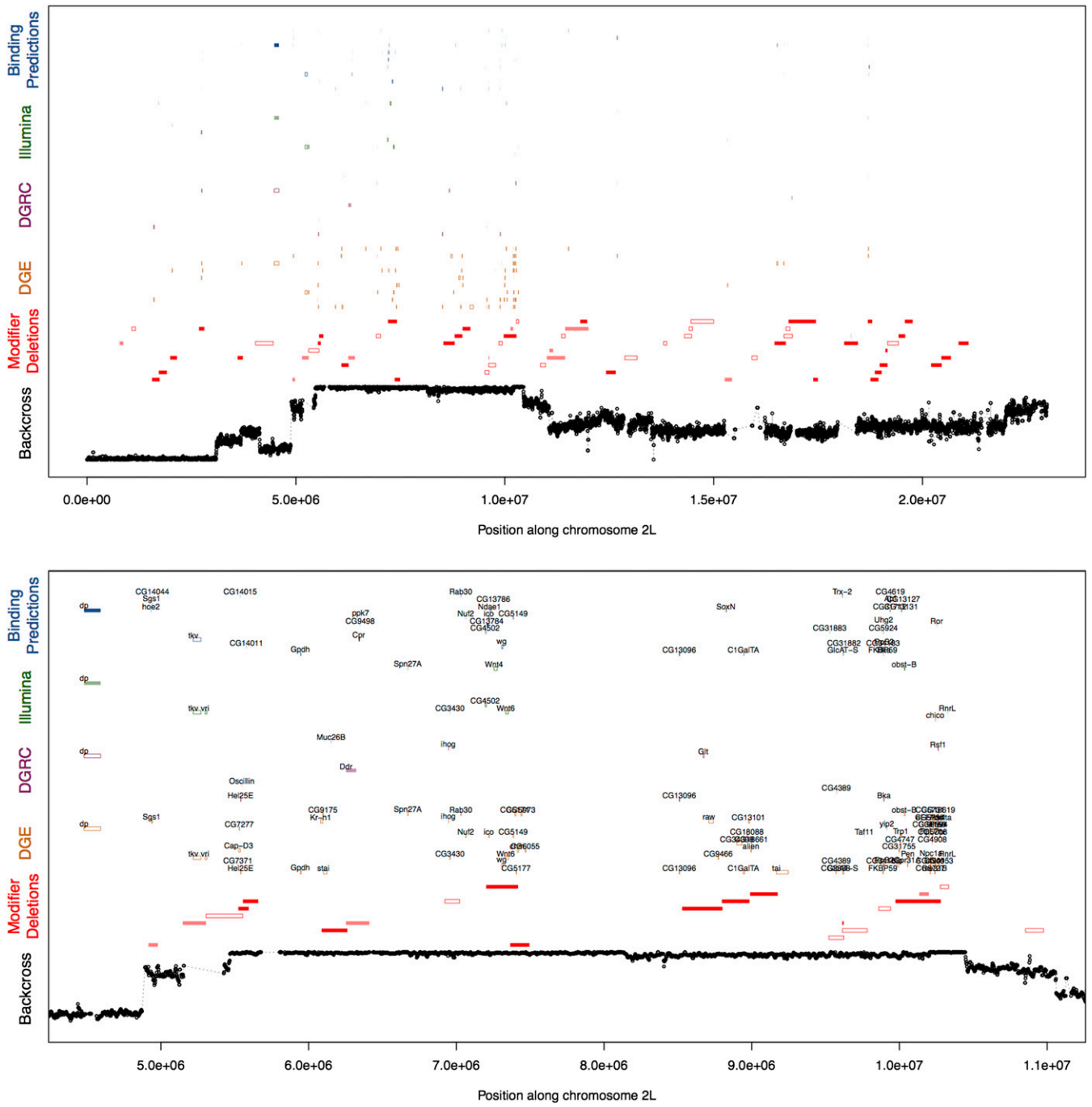

Figure 6 Integration of multiple genomic datasets to generate a narrow set of candidate loci influencing background dependence of *sd*^{E3}. Examples of integrated plots showing results of independent genomic datasets used to investigate the genetic basis of background dependence of the *sd*^{E3} phenotype. Backcross: Average frequency of the ORE (short wing) allele across four short-wing introgression lines. Modifier deletions: Open bars represent deletions with a significant main effect on the *sd*^{E3} phenotype; light shaded bars represent deletions with a significant background-dependent effect on the *sd*^{E3} phenotype; and dark shaded bars represent deletions in which both the main and interaction effects are significant. DGE: Open bars represent genes whose transcript counts are influenced by *sd* genotype; light shaded bars represent genes showing evidence of genotype-dependent allelic imbalance; and dark shaded bars represent genes showing evidence of both an overall effect of *sd* genotype and genotype-dependent allelic imbalance. DGRC and Illumina: Open bars represent genes showing evidence of an effect of *sd* genotype on expression; light shaded bars represent genes showing evidence of a genotype-by-background interaction effect; and dark shaded bars represent genes showing evidence of both the main and interaction effects. Binding predictions: Open bars represent genes predicted to be overall SD binding targets (in at least one of the two genetic backgrounds); light shaded bars represent genes predicted to show differential affinity for SD between the two backgrounds; and dark shaded bars represent genes showing evidence of both overall SD binding and differential affinity between backgrounds. Only genes showing evidence of at least four significant effects across all datasets are shown.

Table 4 Candidate genes identified by integrative analysis of gene expression, sequence binding predictions, and mapping and modifier datasets

Gene name	Chr	Position	Evidence
Prosap	2R	9947961–10028407	Expression, introgression, modifier deletions, binding predictions
CG9427	3R	5450879–5452652	Expression, introgression, modifier deletions
eca	3R	5510191–5511198	Expression, introgression, modifier deletions, binding predictions
ihog	2L	6945464–6948808	Expression, introgression, modifier deletions
obst-B	2L	10032690–10038954	Expression, introgression, modifier deletions
lola	2R	6369399–6430796	Expression, introgression, modifier deletions, binding predictions
sbb	2R	14165703–14244801	Expression, introgression, modifier deletions
vg	2R	8772137–8786890	Expression, introgression, modifier deletions
Vps45	3R	5389646–5391814	Expression, introgression, modifier deletions, binding predictions
pont	3R	6087845–6089621	Expression, introgression, modifier deletions
CG17230	3R	7263507–7293094	Expression, introgression, modifier deletions, binding predictions

also have been influenced by polymorphisms between the SAM and ORE sequences and the probe sequences.

Allelic imbalance

There was very little overlap between genes showing evidence of allelic imbalance in SAM/ORE hybrid flies, genes showing evidence of background-dependent expression levels in pure SAM and ORE flies, and genes containing polymorphic predicted *scalloped* binding sites. The lack of overlap between the first two sets of genes is not surprising, because allelic imbalance must be due to *cis*-regulatory variation, whereas expression differences between pure SAM and ORE flies may be due to either *cis*- or *trans*-regulatory differences. Moreover, our ability to detect allelic imbalance in the DGE dataset was limited by our ability to identify SNPs in our relatively short sequence tags, and by a lack of statistical power for low-abundance transcripts. The comparison between genes showing allelic imbalance and genes predicted to have polymorphic SD binding sites is further hindered by imperfect binding site predictions, and because TFBS can reside quite far from the gene they regulate. The lack of strong congruence between these datasets is therefore also unsurprising.

Interestingly, a large proportion of genes displaying evidence of allelic imbalance showed differences between the wild-type and mutant genotypes: many of the genes showing evidence of allelic imbalance in wild-type flies did not show allelic imbalance in mutant flies, and vice versa (Figure 5, Figure S3). Nevertheless, there did not appear to be any consistent bias in the expression of one background's alleles over the other, nor did there to appear to be any change in the overall degree of allelic imbalance between wild-type and sd^{E3} flies (Figure 5, Figure S3). The latter finding is somewhat surprising, given that we might expect reduced SD levels in sd^{E3} flies to minimize the impact of polymorphic SD binding sites on the expression of SD target genes. However, this analysis was also limited by small sample size; we only had polymorphic sequence tags for a handful of genes, and many of these were expressed at low levels. Larger-scale RNA-seq experiments with longer reads capable of distinguishing alleles will be able to shed more light on this matter. Combined, though, the overall picture that emerges from the binding site and allelic imbalance analyses suggests that *cis*-regulatory variants between SAM and ORE contribute little to the background dependence of the sd^{E3} phenotype, and that variation in *trans*-acting factors may be more important.

Candidate genes

We identified several loci for further study (Table 4). This list contains a number of genes for which a role in wing phenotypes is logical based on prior evidence (*e.g.*, *vg*, *sbb*, *bi/Omb*, *dlg1*, *ban*), suggesting that our approach is selecting a reasonable list of candidate genes. The presence of several genes with little or no experimental evidence for a function in wing development (*e.g.*, *msk*, *obst-B*) shows that this strategy is also capable of detecting novel candidates. This is a key point if our goal is to develop a detailed, unbiased picture of the genetic networks underlying phenotypic variation.

Conclusions

The genetic basis of variation in the penetrance and expressivity of mutations is likely to be complex. Dissecting the genetic basis of this background dependence will require an integrative approach, because precisely mapping alleles with small quantitative effects is difficult, even in well-developed model species like *D. melanogaster*. Drawing on data from multiple experiments with distinct approaches, we have identified a robust set of candidate genes for further investigation as possible factors underlying the background dependence of $scalloped^{E3}$'s variable phenotypic effects on the *D. melanogaster* wing. This approach should prove useful in understanding how genetic background interacts with specific mutations to influence organismal phenotypes.

Acknowledgments

We thank Casey Bergman, Titus Brown, and Greg Gibson for valuable discussions on analyses and for helpful suggestions on earlier versions of this manuscript. This work was supported by National Science Foundation (NSF) MCB-0922344 (to I.D.). This material is based in part upon work

supported by the NSF under cooperative agreement no. DBI-0939454. Any opinions, findings, and conclusions or recommendations expressed in this material are those of the author(s) and do not necessarily reflect the views of the National Science Foundation. The authors declare that they have no competing interests.

Literature Cited

Altenburg, E., and H. J. Muller, 1920 The genetic basis of truncate wing,—an inconstant and modifiable character in *Drosophila*. Genetics 5: 1–59.

Antonov, A. V., 2011 BioProfiling.de: analytical web portal for high-throughput cell biology. Nucleic Acids Res. 39: W323–W327.

Atallah, J., I. Dworkin, U. Cheung, A. Greene, B. Ing *et al.*, 2004 The environmental and genetic regulation of *obake* expressivity: morphogenetic fields as evolvable systems. Evol. Dev. 6: 114–122.

Bailey, T. L., M. Boden, F. A. Buske, M. Frith, C. E. Grant *et al.*, 2009 MEME SUITE: tools for motif discovery and searching. Nucleic Acids Res. 37: W202–W208.

Bray, S., 1999 Drosophila development: Scalloped and Vestigial take wing. Curr. Biol. 9: R245–R247.

Burnett, C., S. Valentini, F. Cabreiro, M. Goss, and M. Somogyvári *et al*. 2011 Absence of effects of *Sir2* overexpression on lifespan in *C. elegans* and *Drosophila*. Nature 477: 482–485.

Cagliero, J., A. Forget, E. Daldello, J. Silber, and A. Zider, 2013 The Hippo kinase promotes Scalloped cytoplasmic localization independently of Warts in a CRM1/Exportin1-dependent manner in *Drosophila*. FASEB J. 27: 1330–1341.

Campbell, S., M. Inamdar, V. Rodrigues, V. Raghavan, M. Palazzolo *et al.*, 1992 The *scalloped* gene encodes a novel, evolutionarily conserved transcription factor required for sensory organ differentiation in *Drosophila*. Genes Dev. 6: 367–379.

Cavicchi, S., D. Guerra, V. Natali, G. Giorgi, C. Pezzoli *et al.*, 1989 Developmental effects of modifiers of the *vg* mutant in *Drosophila melanogaster*. Dev. Genet. 10: 386–392.

Chandler, C. H., 2010 Cryptic intraspecific variation in sex determination in *Caenorhabditis elegans* revealed by mutations. Heredity 105: 473–482.

Chandler, C. H., S. Chari, and I. Dworkin, 2013 Does your gene need a background check? How genetic background impacts the analysis of mutations, genes, and evolution. Trends Genet. 29: 358–366.

Chari, S., and I. Dworkin, 2013 The conditional nature of genetic interactions: the consequences of wild-type backgrounds on mutational interactions in a genome-wide modifier screen. PLoS Genet. 9: e1003661.

Debat, V., A. Debelle, and I. Dworkin, 2009 Plasticity, canalization, and developmental stability of the *Drosophila* wing: joint effects of mutations and developmental temperature. Evolution 63: 2864–2876.

Doggett, K., F. A. Grusche, H. E. Richardson, and A. M. Brumby, 2011 Loss of the *Drosophila* cell polarity regulator Scribbled promotes epithelial tissue overgrowth and cooperation with oncogenic Ras-Raf through impaired Hippo pathway signaling. BMC Dev. Biol. 11: 57.

Dowell, R. D., O. Ryan, A. Jansen, D. Cheung, S. Agarwala *et al.*, 2010 Genotype to phenotype: a complex problem. Science 328: 469.

Duveau, F., and M.-A. Félix, 2012 Role of pleiotropy in the evolution of a cryptic developmental variation in *Caenorhabditis elegans*. PLoS Biol. 10: e1001230.

Dworkin, I., and G. Gibson, 2006 Epidermal growth factor receptor and transforming growth factor-beta signaling contributes to variation for wing shape in *Drosophila melanogaster*. Genetics 173: 1417–1431.

Dworkin, I., A. Palsson, K. Birdsall, and G. Gibson, 2003 Evidence that *Egfr* contributes to cryptic genetic variation for photoreceptor determination in natural populations of *Drosophila melanogaster*. Curr. Biol. 13: 1888–1893.

Dworkin, I., E. Kennerly, D. Tack, J. Hutchinson, J. Brown *et al.*, 2009 Genomic consequences of background effects on *scalloped* mutant expressivity in the wing of *Drosophila melanogaster*. Genetics 181: 1065–1076.

Dworkin, I., J. Anderson, Y. Idaghdour, E. Parker, E. Stone *et al.*, 2011 The effects of weak genetic perturbations on the transcriptome of the wing imaginal disc, and its association with wing shape in *Drosophila melanogaster*. Genetics 187: 1171–1184.

Earley, E. J., and C. D. Jones, 2011 Next-generation mapping of complex traits with phenotype-based selection and introgression. Genetics 189: 1203–1209.

Félix, M., 2007 Cryptic quantitative evolution of the vulva intercellular signaling network in *Caenorhabditis*. Curr. Biol. 17: 103–114.

Gerke, J., K. Lorenz, S. Ramnarine, and B. Cohen, 2010 Gene-environment interactions at nucleotide resolution. PLoS Genet. 6: e1001144.

Gibson, G., M. Wemple, and S. van Helden, 1999 Potential variance affecting homeotic *Ultrabithorax* and Antennapedia phenotypes in *Drosophila melanogaster*. Genetics 151: 1081–1091.

Goulev, Y., J. D. Fauny, B. Gonzalez-Marti, D. Flagiello, J. Silber *et al.*, 2008 SCALLOPED interacts with YORKIE, the nuclear effector of the hippo tumor-suppressor pathway in *Drosophila*. Curr. Biol. 18: 435–441.

Guss, K. A., M. Benson, N. Gubitosi, K. Brondell, K. Broadie *et al.*, 2013 Expression and function of scalloped during *Drosophila* development. Dev. Dyn. 242: 874–885.

Guss, K. A., C. E. Nelson, A. Hudson, M. E. Kraus, and S. B. Carroll, 2001 Control of a genetic regulatory network by a selector gene. Science 292: 1164–1167.

Halder, G., and S. B. Carroll, 2001 Binding of the Vestigial cofactor switches the DNA-target selectivity of the Scalloped selector protein. Development 128: 3295–3305.

Halder, G., P. Polaczyk, M. E. Kraus, A. Hudson, J. Kim *et al.*, 1998 The Vestigial and Scalloped proteins act together to directly regulate wing-specific gene expression in *Drosophila*. Genes Dev. 12: 3900–3909.

Hofmann, A., A. Keinhorst, A. Krumm, and G. Korge, 1987 Regulatory sequences of the Sgs-4 gene of *Drosophila melanogaster* analysed by P element-mediated transformation. Chromosoma 96: 8–17.

Hofmanova, J., 1975 Effect of the genetic background on recombination frequency in the *cn-vg* region of the second chromosome of natural populations of *Drosophila melanogaster*. Folia Biol. 21: 50–59.

Kim, J., R. Cunningham, B. James, S. Wyder, J. D. Gibson *et al.*, 2010 Functional characterization of transcription factor motifs using cross-species comparison across large evolutionary distances. PLOS Comput. Biol. 6: e1000652.

King, E. G., C. M. Merkes, C. L. McNeil, S. R. Hoofer, S. Sen *et al.*, 2012 Genetic dissection of a model complex trait using the *Drosophila* Synthetic Population Resource. Genome Res. 22: 1558–1566.

Koontz, L. M., Y. Liu-Chittenden, F. Yin, Y. Zheng, J. Yu *et al.*, 2013 The *hippo* effector *yorkie* controls normal tissue growth by antagonizing scalloped-mediated default repression. Dev. Cell 25: 388–401.

Lalić, J., and S. F. Elena, 2013 Epistasis between mutations is host-dependent for an RNA virus. Biol. Lett. 9: 20120396.

Leips, J., and T. F. C. Mackay, 2002 The complex genetic architecture of *Drosophila* life span. Exp. Aging Res. 28: 361–390.

Li, H., and R. Durbin, 2009 Fast and accurate short read alignment with Burrows-Wheeler transform. Bioinformatics 25: 1754–1760.

Li, H., B. Handsaker, A. Wysoker, T. Fennell, J. Ruan, N. Homer, G. Marth, G. Abecasis, and R. Durbin; 1000 Genome Project Data

Processing Subgroup, 2009 The Sequence Alignment/Map format and SAMtools. Bioinformatics 25: 2078–2079.
Lyman, R. F., and T. F. Mackay, 1998 Candidate quantitative trait loci and naturally occurring phenotypic variation for bristle number in *Drosophila melanogaster*: the Delta-Hairless gene region. Genetics 149: 983–998.
Lyman, R. F., F. Lawrence, S. V. Nuzhdin, and T. F. Mackay, 1996 Effects of single P-element insertions on bristle number and viability in *Drosophila melanogaster*. Genetics 143: 277–292.
Mackay, T. F. C., R. F. Lyman, and F. Lawrence, 2005 Polygenic mutation in *Drosophila melanogaster*: mapping spontaneous mutations affecting sensory bristle number. Genetics 170: 1723–1735.
Mackenzie, D. K., L. F. Bussiere, and M. C. Tinsley, 2011 Senescence of the cellular immune response in *Drosophila melanogaster*. Exp. Gerontol. 46: 853–859.
McGuigan, K., N. Nishimura, M. Currey, D. Hurwit, and W. A. Cresko, 2011 Cryptic genetic variation and body size evolution in threespine stickleback. Evolution 65: 1203–1211.
McKenzie, J. A., M. J. Whitten, and M. A. Adena, 1982 The effect of genetic background on the fitness of diazinon resistance genotypes of the Australian sheep blowfly, *Lucilia cuprina*. Heredity 49: 1–9.
Milloz, J., F. Duveau, I. Nuez, and M.-A. Felix, 2008 Intraspecific evolution of the intercellular signaling network underlying a robust developmental system. Genes Dev. 22: 3064–3075.
Morrissy, A. S., R. D. Morin, A. Delaney, T. Zeng, H. McDonald *et al.*, 2009 Next-generation tag sequencing for cancer gene expression profiling. Genome Res. 19: 1825–1835.
Nakashima-Tanaka, E., 1967 The effect of temperature and genetic background on the phenotypic expression of several Vestigial strains of *Drosophila melanogaster*. Genetica 38: 447–458.
Nicolay, B. N., B. Bayarmagnai, A. B. M. M. K. Islam, N. Lopez-Bigas, and M. V. Frolov, 2011 Cooperation between dE2F1 and Yki/Sd defines a distinct transcriptional program necessary to bypass cell cycle exit. Genes Dev. 25: 323–335.
Palsson, A., and G. Gibson, 2000 Quantitative developmental genetic analysis reveals that the ancestral dipteran wing vein prepattern is conserved in *Drosophila melanogaster*. Dev. Genes Evol. 210: 617–622.
Paumard-Rigal, S., A. Zider, P. Vaudin, and J. Silber, 1998 Specific interactions between vestigial and scalloped are required to promote wing tissue proliferation in *Drosophila melanogaster*. Dev. Genes Evol. 208: 440–446.
Polaczyk, P. J., R. Gasperini, and G. Gibson, 1998 Naturally occurring genetic variation affects *Drosophila* photoreceptor determination. Dev. Genes Evol. 207: 462–470.
Poon, C. L. C., X. Zhang, J. I. Lin, S. A. Manning, and K. F. Harvey, 2012 Homeodomain-interacting protein kinase regulates Hippo pathway-dependent tissue growth. Curr. Biol. 22: 1587–1594.
Ray, A., W. V. D. G. van Naters, and J. R. Carlson, 2008 A regulatory code for neuron-specific odor receptor expression. PLoS Biol. 6: e125.
Remold, S. K., and R. E. Lenski, 2004 Pervasive joint influence of epistasis and plasticity on mutational effects in *Escherichia coli*. Nat. Genet. 36: 423–426.
Ren, F., L. Zhang, and J. Jiang, 2010 Hippo signaling regulates Yorkie nuclear localization and activity through 14–3-3 dependent and independent mechanisms. Dev. Biol. 337: 303–312.
Robinson, M. D., D. J. McCarthy, and G. K. Smyth, 2010 edgeR: a Bioconductor package for differential expression analysis of digital gene expression data. Bioinformatics 26: 139–140.
Ross, J. A., D. C. Koboldt, J. E. Staisch, H. M. Chamberlin, B. P. Gupta *et al.*, 2011 *Caenorhabditis briggsae* recombinant inbred line genotypes reveal inter-strain incompatibility and the evolution of recombination. PLoS Genet. 7: e1002174.
Seidel, H. S., M. V. Rockman, and L. Kruglyak, 2008 Widespread genetic incompatibility in *C. elegans* maintained by balancing selection. Science 319: 589–594.
Shyamala, B. V., and A. Chopra, 1999 *Drosophila melanogaster* chemosensory and muscle development: identification and properties of a novel allele of *scalloped* and of a new locus, SG18.1, in a Gal4 enhancer trap screen. J. Genet. 78: 87–97.
Sidor, C. M., R. Brain, and B. J. Thompson, 2013 Mask proteins are cofactors of Yorkie/YAP in the Hippo pathway. Curr. Biol. 23: 223–228.
Silber, J., 1980 Penetrance of the *vestigial* gene in *Drosophila melanogaster*. Genetica 54: 91–99.
Simmonds, A. J., X. Liu, K. H. Soanes, H. M. Krause, K. D. Irvine *et al.*, 1998 Molecular interactions between Vestigial and Scalloped promote wing formation in *Drosophila*. Genes Dev. 12: 3815–3820.
Storey, J. D., and R. Tibshirani, 2003 Statistical significance for genomewide studies. Proc. Natl. Acad. Sci. USA 100: 9440–9445.
Tanaka, E., 1960 A study on the difference of temperature responses in several *vestigial* strains of *Drosophila melanogaster*. Jpn. J. Genet. 35: 222–227.
Thompson, J. N., 1975 Studies on the nature and function of polygenic loci in *Drosophila*. III. Veinlet modifiers having region-specific effects upon the vein pattern. Genetics 81: 387–402.
Threadgill, D. W., A. A. Dlugosz, L. A. Hansen, T. Tennenbaum, U. Lichti *et al.*, 1995 Targeted disruption of mouse EGF receptor: effect of genetic background on mutant phenotype. Science 269: 230–234.
Vaistij, F. E., Y. Gan, S. Penfield, A. D. Gilday, A. Dave *et al.*, 2013 Differential control of seed primary dormancy in *Arabidopsis* ecotypes by the transcription factor SPATULA. Proc. Natl. Acad. Sci. USA 110: 10866–10871.
Varadarajan, S., and K. VijayRaghavan, 1999 *scalloped* functions in a regulatory loop with *vestigial* and *wingless* to pattern the *Drosophila* wing. Dev. Genes Evol. 209: 10–17.
Wang, J., D. Duncan, Z. Shi, and B. Zhang, 2013a WEB-based GEne SeT AnaLysis Toolkit (WebGestalt): update 2013. Nucleic Acids Res. 41: W77–W83.
Wang, Y., C. D. Arenas, D. M. Stoebel, and T. F. Cooper, 2013b Genetic background affects epistatic interactions between two beneficial mutations. Biol. Lett. 9: 20120328.
Weinreich, D. M., Y. Lan, C. S. Wylie, and R. B. Heckendorn, 2013 Should evolutionary geneticists worry about higher-order epistasis? Curr. Opin. Genet. Dev. 23: 700–707.
Whitlock, M. C., and D. Bourguet, 2000 Factors affecting the genetic load in *Drosophila*: synergistic epistasis and correlations among fitness components. Evolution 54: 1654–1660.
Wu, S., Y. Liu, Y. Zheng, J. Dong, and D. Pan, 2008 The TEAD/TEF family protein Scalloped mediates transcriptional output of the Hippo growth-regulatory pathway. Dev. Cell 14: 388–398.
Xu, J., G. Gontier, Z. Chaker, P. Lacube, and J. Dupont *et al.*, 2013 Longevity effect of IGF-1R(+/−) mutation depends on genetic background-specific receptor activation. Aging Cell 13: 19–28.
Zhang, L., F. Ren, Q. Zhang, Y. Chen, B. Wang *et al.*, 2008 The TEAD/TEF family of transcription factor Scalloped mediates Hippo signaling in organ size control. Dev. Cell 14: 377–387.
Zhang, X., C. C. Milton, P. O. Humbert, and K. F. Harvey, 2009 Transcriptional output of the Salvador/warts/hippo pathway is controlled in distinct fashions in *Drosophila melanogaster* and mammalian cell lines. Cancer Res. 69: 6033–6041.
Zhang, X., C. C. Milton, C. L. C. Poon, W. Hong, and K. F. Harvey, 2011 Wbp2 cooperates with Yorkie to drive tissue growth downstream of the Salvador-Warts-Hippo pathway. Cell Death Differ. 18: 1346–1355.
Zhang, Z., B. Hsieh, A. Poe, J. Anderson, K. Ocorr *et al.*, 2013 Complex genetic architecture of cardiac disease in a wild-type inbred strain of *Drosophila melanogaster*. PLoS ONE 8: e62909.
Zhao, B., X. Ye, J. Yu, L. Li, W. Li *et al.*, 2008 TEAD mediates YAP-dependent gene induction and growth control. Genes Dev. 22: 1962–1971.

Communicating editor: C. Jones

GENETICS

Supporting Information
http://www.genetics.org/lookup/suppl/doi:10.1534/genetics.113.159426/-/DC1

Causes and Consequences of Genetic Background Effects Illuminated by Integrative Genomic Analysis

Christopher H. Chandler, Sudarshan Chari, David Tack, and Ian Dworkin

DOI: 10.1534/genetics.113.159426

Table S1 Known SD binding site sequences used to generate position weight matrix to scan the SAM and ORE genomes for predicted SD binding sites.

Gene	Coordinates	Sequence	Source
ct	X:7424390..7424403	TTTGTGAATGAAGT	REDfly TF000140
ct	X:7424422..7424433	TAACATTTAATT	REDfly TF000139
ct	X:7424473..7424487	GATAAACAGCAGTGT	REDfly TF000138
ct	X:7424494..7424520	GCTGTTTTTTTAAATGAATTTTCTCTA	REDfly TF000137
ct	X:7424594..7424610	AAAATTATTGAAATTAC	REDfly TF000136
ct	X:7424692..7424701	GGAATGGGAT	REDfly TF000135
ct	X:7424821..7424843	AATGTAATTCGAAAAATGTCGTC	REDfly TF000134
vg	2R:8782964..8783003	GCTAGTTGGAATGTGCTATGAAATGTCGCCGGAATGCGAT	REDfly TF001715
vg	2R:8783977..8783987	GGAAATATCTT	REDfly TF000458
vg	2R:8784014..8784027	TGGGAATTCCACGG	REDfly TF000459
vg	2R:8784101..8784114	CACGCGGCATGGCA	REDfly TF000460
vg	2R:8784375..8784386	GTTTGGAATGTT	REDfly TF000465
bs	2R:20229832..20229857	TAAGAAATTCCTGGCATAGTTTAAGT	REDfly TF000512
salm	2L:11454576..11454582	TATGCGA	REDfly TF000032
salm	2L:11454656..11454679	AATGGACATTCGTGGGATTCCAGA	REDfly TF001599
salm	2L:11454657..11454680	ATGGACATTCGTGGGATTCCAGAA	REDfly TF000029
salm	2L:11454657..11454680	ATGGACATTCGTGGGATTCCAGAA	REDfly TF000030
kni	3L:20700051..20700068	TACATTTGTCGCATAGTT	REDfly TF000811
kni	3L:20700243..20700251	ATACATACA	REDfly TF000812
kni	3L:20700303..20700311	AAAATGTCG	REDfly TF000813
kni	3L:20700350..20700358	GAAATGCGT	REDfly TF000814
kni	3L:20700420..20700428	AGAAATAGT	REDfly TF000815
diap1		GCATTCCATT	Wu et al. 2008

Table S2 Position weight matrix used to scan the SAM and ORE genomes for SD binding sites, derived from a MEME (Bailey et al. 2009) scan of 23 known SD binding sites.

	A	C	G	T
1	0	5	14	4
2	8	1	14	0
3	18	4	0	1
4	22	0	1	0
5	0	0	0	23
6	3	0	14	6
7	3	3	3	14

Table S3 Detailed sequence pile-up (Li et al. 2009) for *scalloped* binding site regulating *cut* (Halder & Carrol 2001, Guss et al. 2001).

Chrom.	Pos.	Ref.	# reads (SAM)	Read bases (SAM)	Base quality (SAM)	# reads (ORE)	Read bases (ORE)	Base quality (ORE)
X	7424817	T	15	,....,,,,,,...	HFIHIDIBI<GIIII	15	.$,.,,.,.,.,.,.	DIIFIIIIIIIHIII
X	7424818	G	15	,....,,,,,,...	HIHGIEIGIGGIIIG	15	,.,,.,.,.,.,.^],	GIIIIIHGIHIIHIE
X	7424819	T	16	,$....,,,,,,...^].	EHGGICHGIGDIIHGE	15	,$.,,.,.,.,.,.,	EIIIIIIIIIIIII
X	7424820	C	15	....,,,,,,....	IIII4IBIBGIIIGI	16	.,,.,.,.,.,.,^],^],	IGGIIIIIIIIBIIEE
X	7424821	A	15	....,,,,,,..G.	IHIICIBIGGIII*I	18	.,,.,.,.,.,.,,,^],^],	IIIIIIIIBIIIIIIDBB
X	7424822	A	15	....,,,,,,....	FHHIEIGIDGIIGGI	18	.,,.,.,.,.,.,,,,,	IIIIIIHIIIIIIHIIEE
X	7424823	T	15	....,,,,,,....	HIIIDIGICGIIIGI	18	.,,.,.,.,.,.,,,,,	IIIIIIIIHHI@IIIGII
X	7424824	G	15	....,,,,,,....	GIIIDI@IEGIGIGI	18	.,,.,.,.,.,.,,,,,	IIIIIIIIDIIIIHIIIG
X	7424825	T	15	.$...,,,,,,....	EGGG=HDICGIIIGI	18	.,,.,.,.,.,.,,,,,	IIIIIIIIIIGIIEHII
X	7424826	A	14	...,,,,,,....	IHIBIGIDGGIIGI	18	.,,.,.,.,.,.,,,,,	IIIIIIIIIIGIIIIII
X	7424827	A	14	...,,,,,,....	HII:I4IDGIIIGI	19	.,,.,.,.,.,.,,,,,^],	IIIIIIIIIIIIIIHIG>
X	7424828	T	14	...,,,,,,....	III=IEIEGIIIII	22	.,,.,.,.,.,.,,,,,^],^],^],	IHIIIIIHIIIIIIIHIIEBBB
X	7424829	T	14	...,,,,,,....	III?IBICDIIIII	23	.,,.,.,.,.,.,,,,,,,^],	IIHIIIFIIHIIIFIFHICEEED
X	7424830	C	14	...,,,,,,....	IIH?IDIDDIIIII	23	.,,.,.,.,.,.,,,,,,,	IIIIIIHIIIIHIGIIIHBFIHF
X	7424831	G	14	.$..,,,,,,....	EDIDIGICGIIIII	24	.,,.,.,.,.,.,,,,,,,^],	IIIIIIIIHIIIIIIIIGBIHIE
X	7424832	A	14	...,,,,,,....^].	>>DFGI>EIIIII7	25	.,,.,.,.,.,.,,,,,,,^].	IIIHIIIGIIIIIIIHGHIGII>
X	7424833	A	14	.$.,,,,,.....	;;<IGIGHIIIII:	25	.,,.,.,.,.,.,,,,,,,.	IIIIIIIIIIHIIIIIDII>II?
X	7424834	A	13	.$,.,,,,.....	9?IBIGHIIIII5	25	.,,.,.,.,.,.,,,,,,,.	IIIIIIIIIIIIIIEIH>IIHIIA
X	7424835	A	12	,.,,,,.....	BIGIDHIHIII5	25	.,,.,.,.,.,.,,,,,,,.	IIIIIIIIIIIIIIIGIHHIIB
X	7424836	A	12	,.,,,,.....	DIGIDHIIIII2	25	.,,.,.,.,.,.,,,,,,,.	IIIGIIIIIIHIHIEIIGIHBIIE
X	7424837	T	12	,.,,,,.....	@IBGBEFBIII-	26	.,,.,.,.,.,.,,,,,,,.^].	IIIIIIIIII8IHHHI@ADHDEDIE
X	7424838	G	12	,.,,,,.....	GIGHDDIIIII:	26	.,,.,.,.,.,.,,,,,,,.	HIIIIIIIHIIIIIIIIGHHHIIII
X	7424839	T	12	,.,,,,.....	GH@IGGHIFHI4	26	.,,.,.,.,.,.,,,,,,,.	HIIIHIIIHIIGIIIIII3IHHIHII
X	7424840	C	12	,.,,,,.....	GIGI<GIIIII5	26	.,,.,.,.,.,.,,,,,,,.	IIIIIIIIIIIIIIHIG8IHDIHII
X	7424841	G	13	,.,,,,.....^].	:IGIGGIIGII7E	26	.,,.,.,.,.,.,,,,,,,.	IIIIIIIIIIIIHIIIIGIIHIIII

Table S4 Detailed sequence pile-up (Li et al. 2009) for *scalloped* binding site regulating *sal* (Guss et al. 2001).

Chrom.	Pos.	Ref.	# reads (SAM)	Read bases (SAM)	Base quality (SAM)	# reads (ORE)	Read bases (ORE)	Base quality (ORE)
2L	11454659	G	17	,,...,..,,,,.,..,	II+IIIIIGIIIIIHII	17	,,..,,.,.,,.,,,,	77977<97777787777
2L	11454660	G	18	,,...,..,,,,.,..,^],	II3IIIIIGIIIIIEIIE	17	,,..,,.,.,,.,,,,	34644964444454444
2L	11454661	A	18	,,...,..,,,,.,..,,	IH6@HIHIBIIIIIIIHH	17	ggGGggGgGggGGgggg	))644964444454444
2L	11454662	C	18	,$,...,..,,,,.,..,,	EI8IIIIIBHIIIIIIII	18	,$,..,,.,.,,.,,,,^>,	))HFF?IIIIIIIIIIC
2L	11454663	A	17	,...,..,,,,.,..,,	I38IIIIGGHIIIHIII	17	,$..,,.,.,,.,,,,,	)HFFDIHIIIIIIIH8
2L	11454664	T	17	,...,..,,,,.,..,,	IBGIIIIGIIIIHHIII	16	.$.$,$,..,,,.,,,,,	>>>DIGIIIHIIGIIC
2L	11454665	T	18	,...,..,,,,.,..,,^],	IAEIIIIGIIIIIIHIE	13	,$.,.,,,.,,,,,	BIIIHIIIIIII?
2L	11454666	C	18	,$...,.,,,,.,.,,,	EAEIIIIGIHHIIGIIIH	12	.,,,,.,,,,,	5GIIIIIIIHI@
2L	11454667	G	17	...,.,,,,.,.,,,	A@IIIIGIIIIGIIIII	13	.,,,,.,,,,,^],	-8888988888?!
2L	11454668	T	17	.$.$.,.,,,,.,.,,,	?BIIIIDIIIII@IFII	13	CcCccCCcccccc	!44445444442!
2L	11454669	G	15	.,.,,,,.,.,,,	IIIIGIIIIIGIHII	13	.,,,.,,,,,,	!3333433333<!
2L	11454670	G	15	.,.,,,,.,.,,,	IIIIBIIIIHGIIII	13	A$aAaaAAaaaaaa	!1111211111;!
2L	11454671	G	15	.,.,,,,.,.,,,	IIIIEIIIIIGIIII	13	,.,,.,,,,,,^>.	7777877777@0E
2L	11454672	A	15	.,.,,,,.,.,,,	IIIIGIIIIIDIIIH	14	,.,,.,,,,,,.^],	IGIIIIIIII46HE
2L	11454673	T	16	.$,$..,,,,.,.,,,^],	>>IIGHIIIIGIIIFB	15	,.,,.,,,,,,.,^],	GIIIIIIHIH;>HIB
2L	11454674	T	14	.,,,,,.,.,,,	IIGIIIIHGIIHIE	15	,.,,.,,,,,,.,,	HIIIIIIEII,<HIE
2L	11454675	C	14	.$.,,,,.,.,,,	>E@IIIIIGIIIFG	15	,.,,.,,,,a,.,,	EIIHIIIIII,IGII
2L	11454676	C	13	.$,,,,.,.,,,	BGIIIIIIIIII	15	,$.,,.,,,,,.,,	BIIIIIIGII;IHII

Table S5 Top 200 genes identified as being differentially expressed between wild-type and sd^{E3} mutant flies by DGE analysis. (See SuppTable5.csv in Dryad package, doi:10.5061/dryad.1375s)

Table S6 Genes showing evidence of allelic imbalance in "hybrid" SAM/ORE flies (i.e., in which one of the two alleles is transcribed at significantly higher levels). (See SuppTable6.csv in Dryad package, doi:10.5061/dryad.1375s)

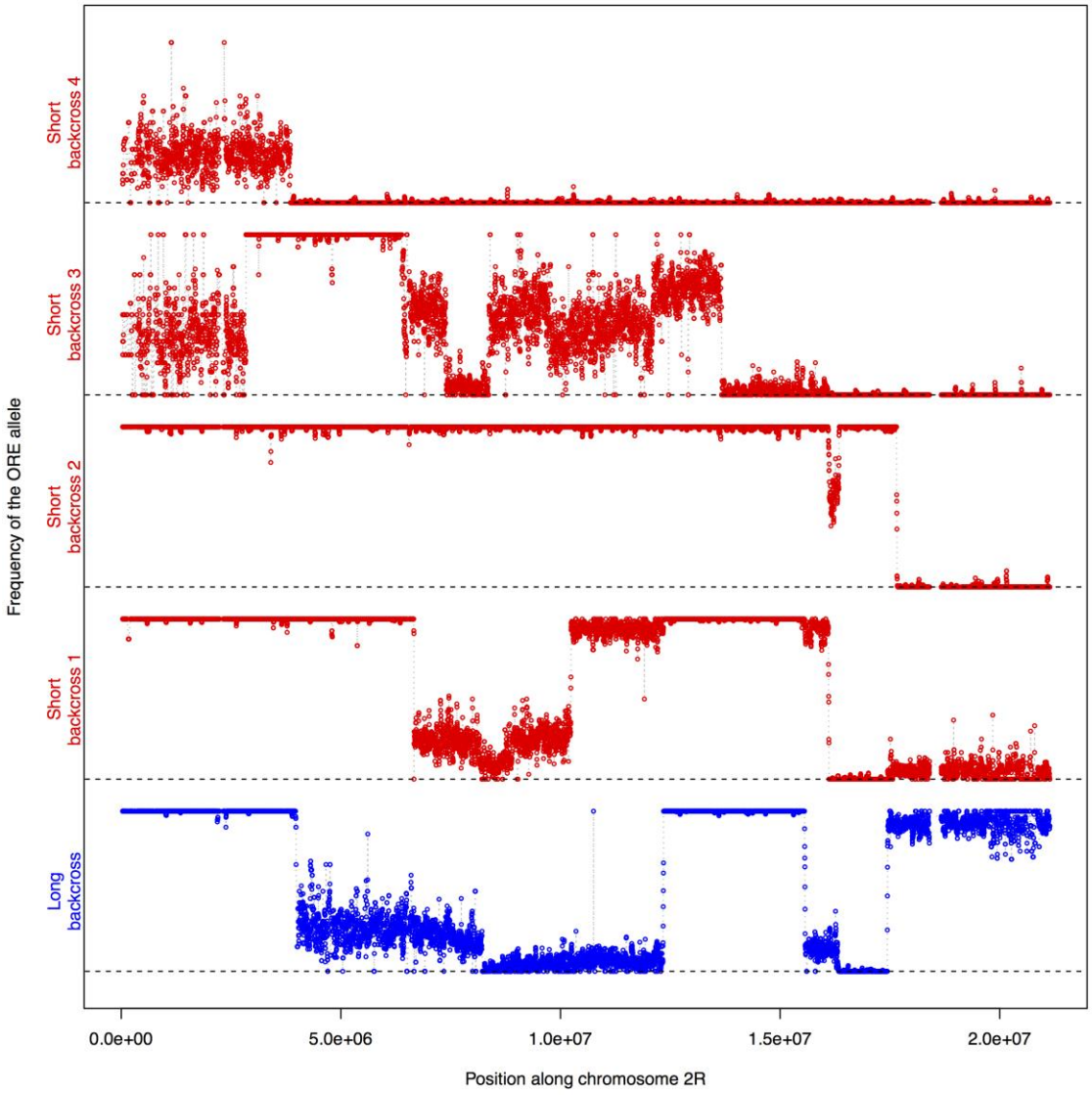
Short backcross 4
Short backcross 3
Short backcross 2
Short backcross 1
Long backcross
Frequency of the ORE allele
0.0e+00
5.0e+06
1.0e+07
1.5e+07
2.0e+07
Position along chromosome 2R

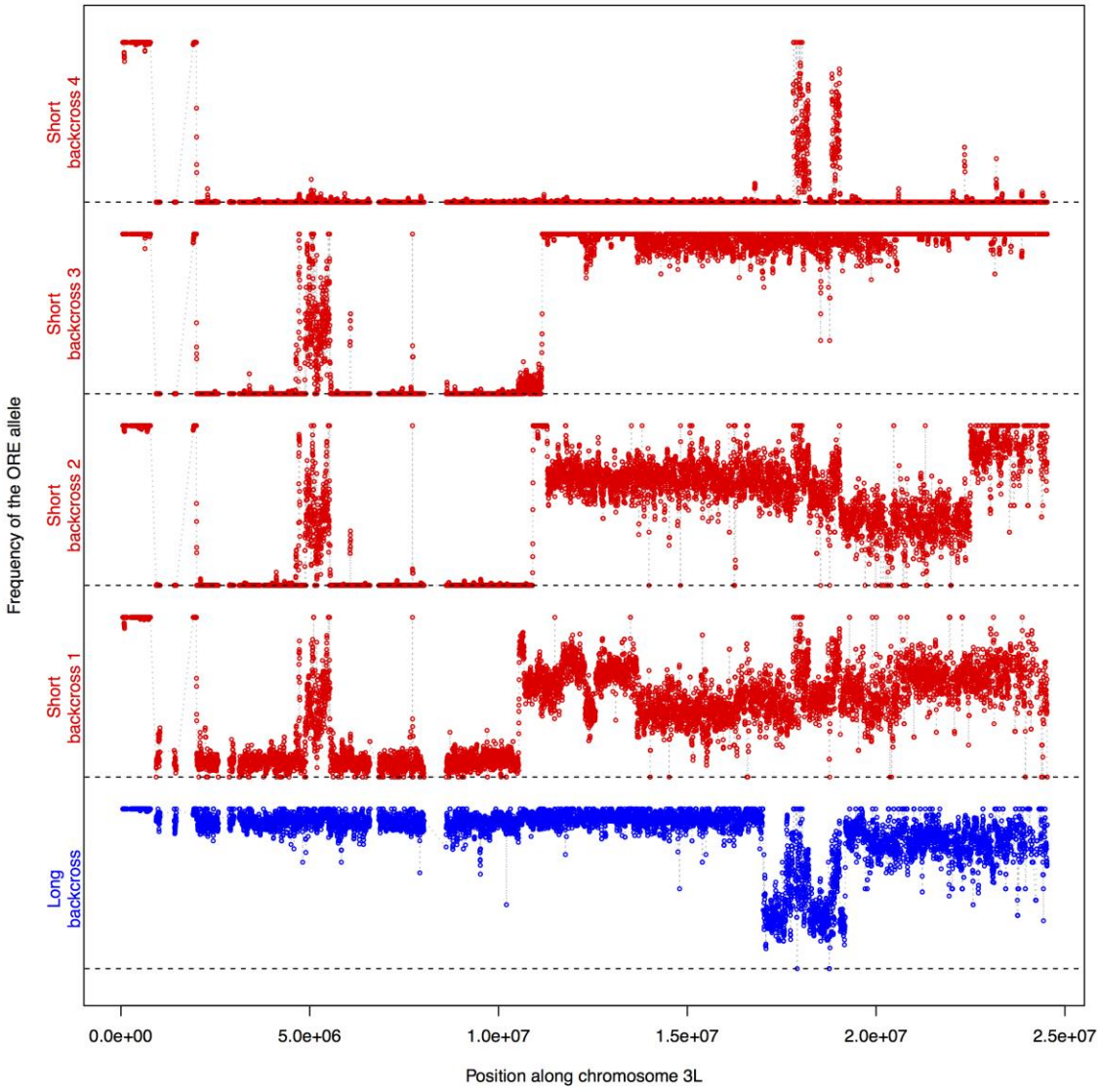
Short backcross 4
Short backcross 3
Short backcross 2
Short backcross 1
Long backcross
Frequency of the ORE allele
0.0e+00
5.0e+06
1.0e+07
1.5e+07
2.0e+07
2.5e+07
Position along chromosome 3L

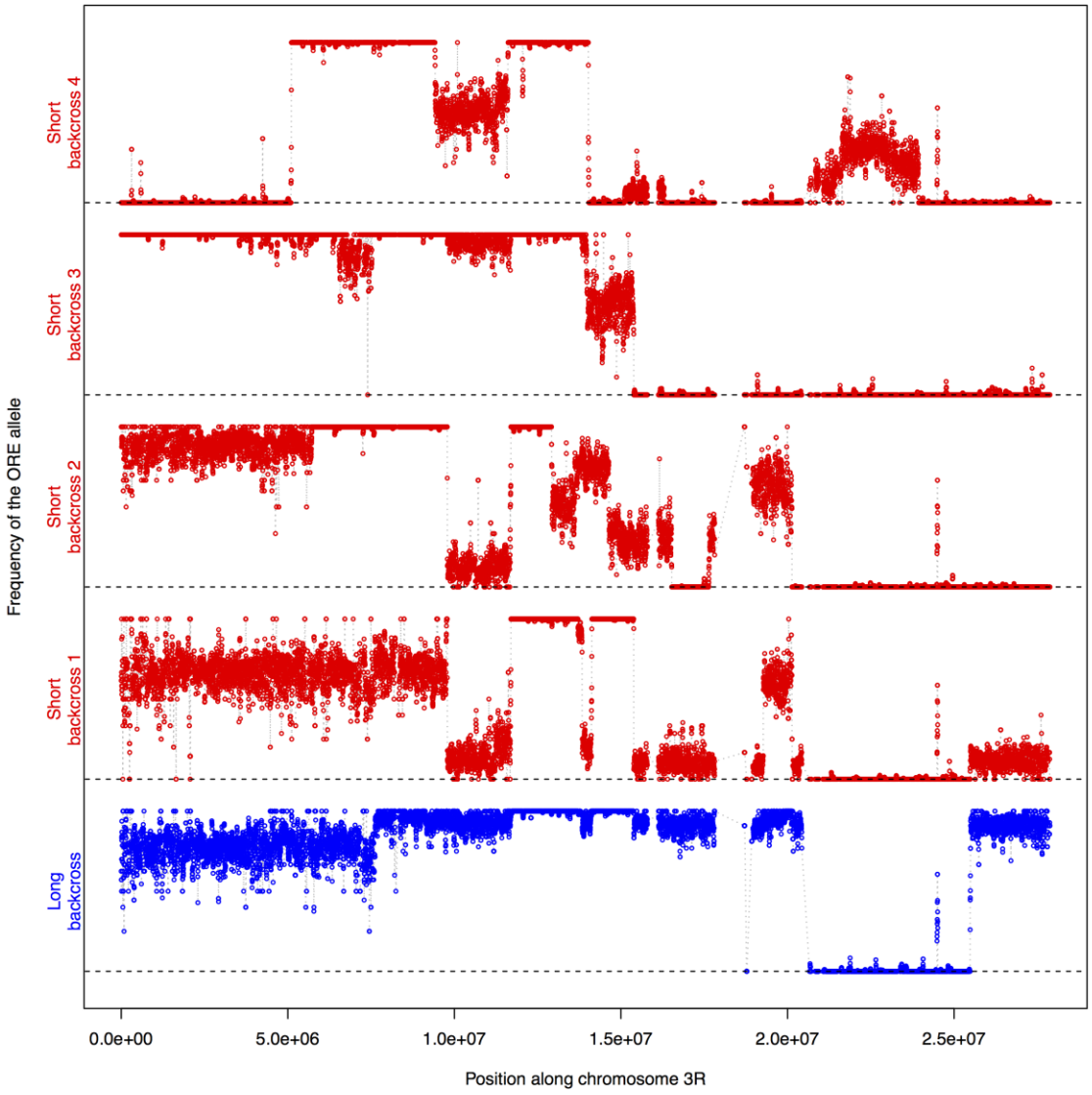

Figure S1 Frequency of the ORE allele along the length of chromosome arms 2R, 3L, and 3R in short- and long-wing *sd*^{E3} backcross lines.

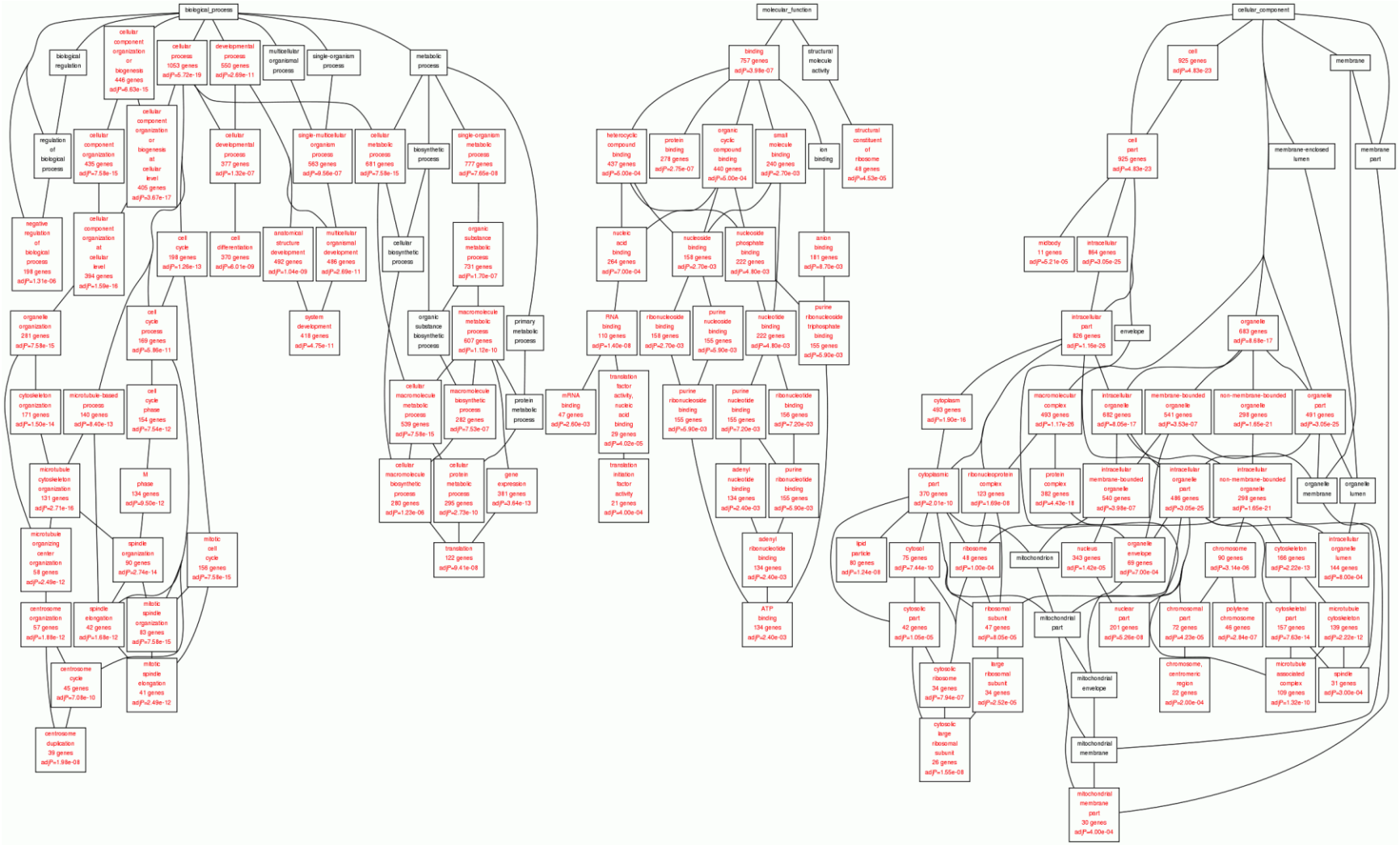

Figure S2 Top hits for GO terms enriched in genes showing evidence of differential expression (q < 0.001) between wild-type and *sd*^{E3} fly wings in the DGE dataset.

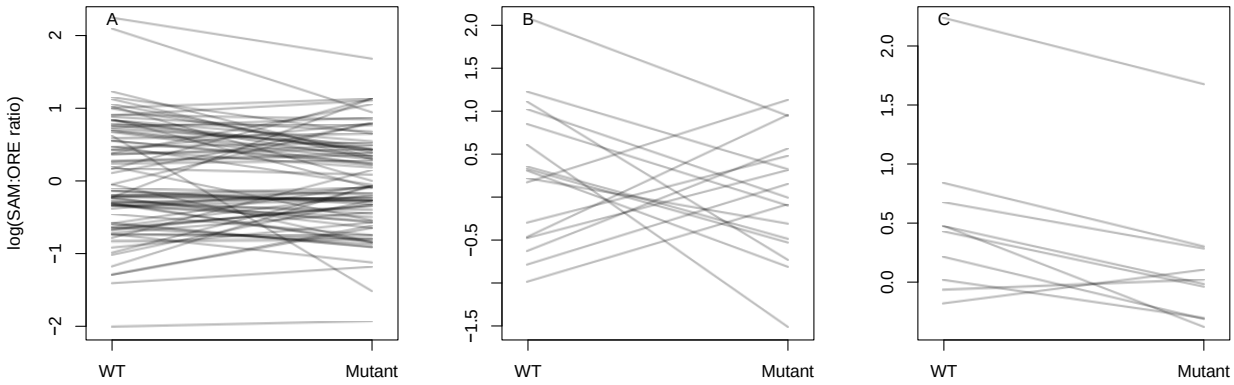

Figure S3 Allelic imbalance in SAM/ORE "hybrid" flies with both wild-type and *sd*^{E3} genotypes. Only sequence tags represented by at least five reads of each allele in all samples are represented in this plot. (A) Genes showing evidence of allelic imbalance ($q < 0.05$). (B) Genes showing evidence of genotype-dependent allelic imbalance ($q < 0.05$). (C) Genes near polymorphic predicted SD binding site ($p < 0.05$).

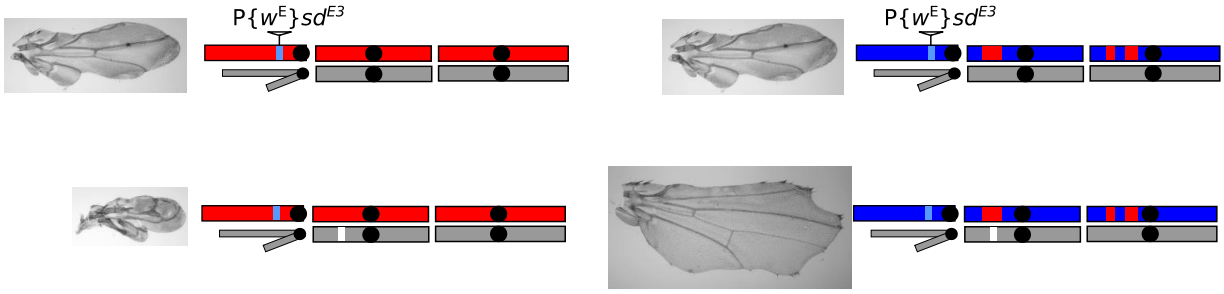

Figure S4 Schematic illustrating tests to distinguish between second- and higher-order epistasis. Red indicates the ORE genetic background; blue indicates the SAM genetic background; grey indicates the genetic background of the deletion strain; white indicates a chromosomal deletion; and the light blue bar on the X chromosome indicates the sd^{E3} allele and the genetic background in which it was originally generated. The genotypes and phenotypes on the left illustrate that this particular deletion enhances the sd^{E3} phenotype in an ORE background, i.e., results in even smaller wings. On the right, however, this deletion suppresses the sd^{E3} phenotype in a short-wing introgression background (i.e., results in larger wings). However, because the short-wing and ORE flies both carry the same genetic background (ORE) opposite the deletion, this background dependence must be due to other loci elsewhere in the genome (in this case, illustrated by the SAM alleles elsewhere in the genome), indicating higher-order epistasis.

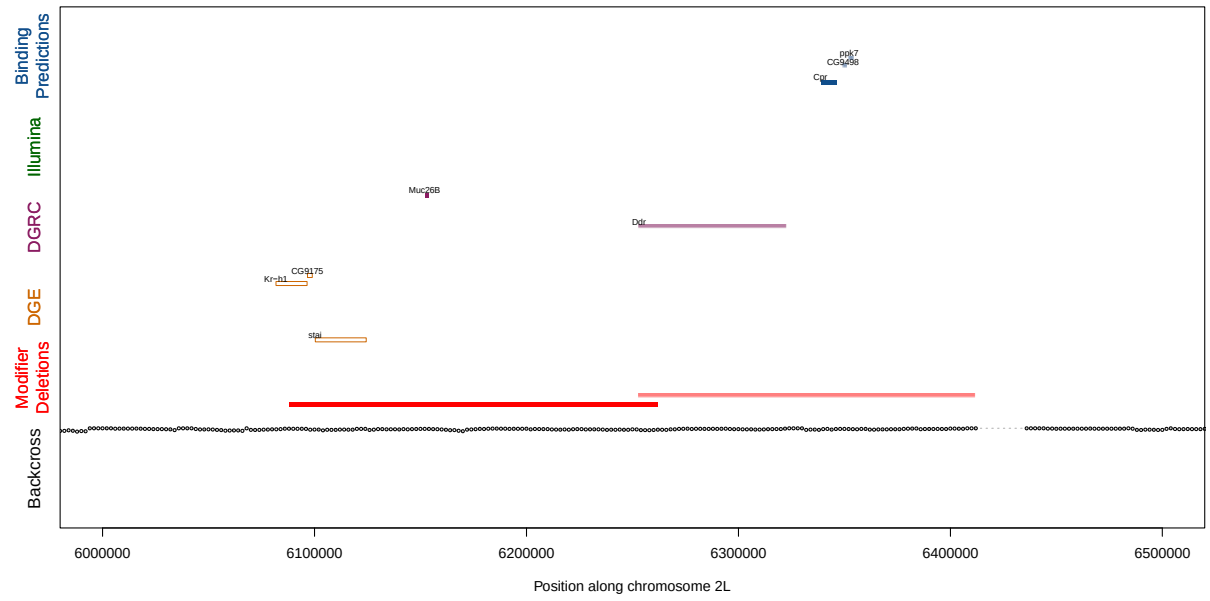
Binding Predictions
Illumina
DGRC
DGE
Modifier Deletions
Backcross
ppk7
CG9498
Cpr
Muc26B
Ddr
Kr-h1
CG9175
stai
6000000
6100000
6200000
6300000
6400000
6500000
Position along chromosome 2L

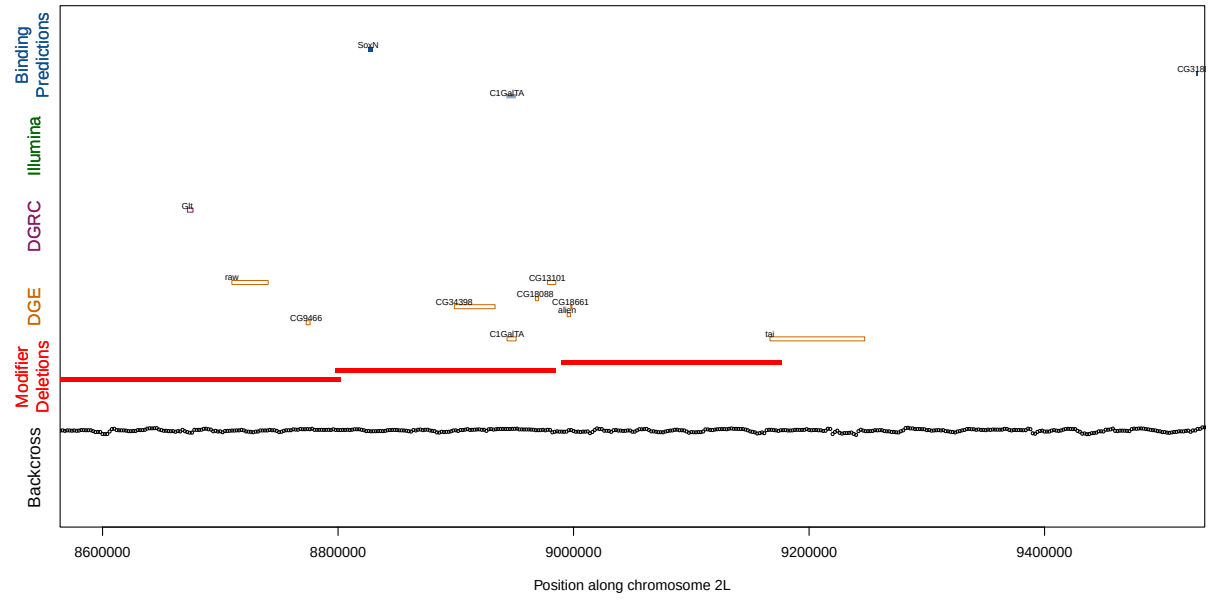
Binding Predictions
Illumina
DGRC
DGE
Modifier Deletions
Backcross
SoxN
C1GalTA
Git
raw
CG13101
CG18088
CG34398
CG18661
allgh
CG9466
C1GalTA
tai
8600000
8800000
9000000
9200000
9400000
Position along chromosome 2L

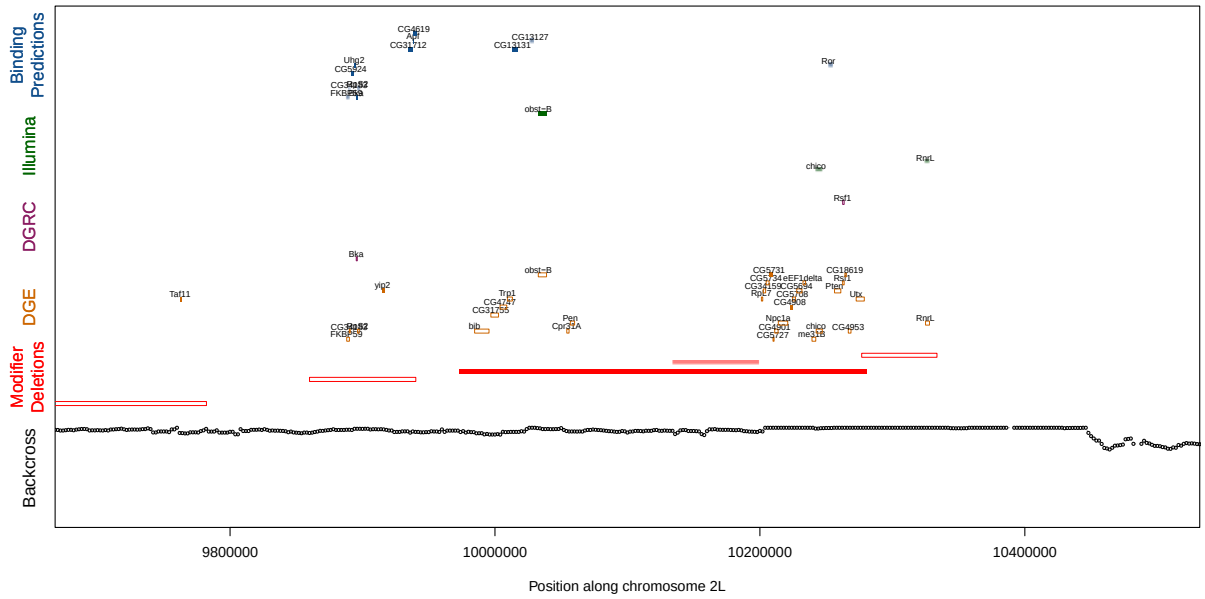
Binding Predictions
Illumina
DGRC
DGE
Modifier Deletions
Backcross
9800000
10000000
10200000
10400000
Position along chromosome 2L

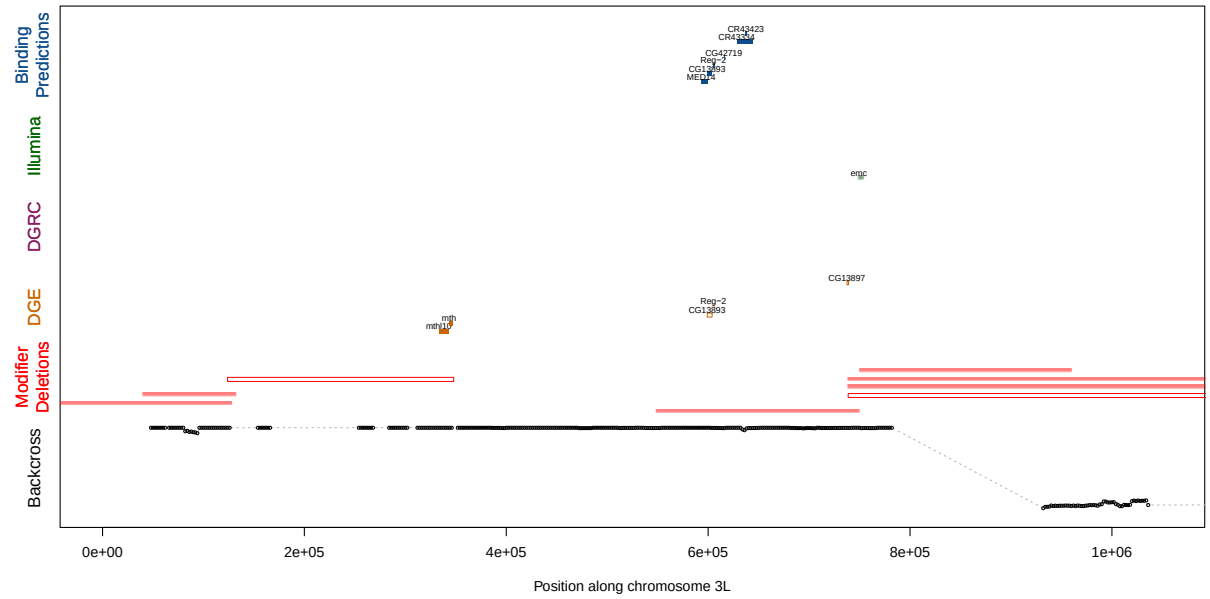
Binding Predictions
Illumina
DGRC
DGE
Modifier Deletions
Backcross
CR43423
CG42719
Reg−2
CG13893
emc
CG13897
mth
0e+00
2e+05
4e+05
6e+05
8e+05
1e+06
Position along chromosome 3L

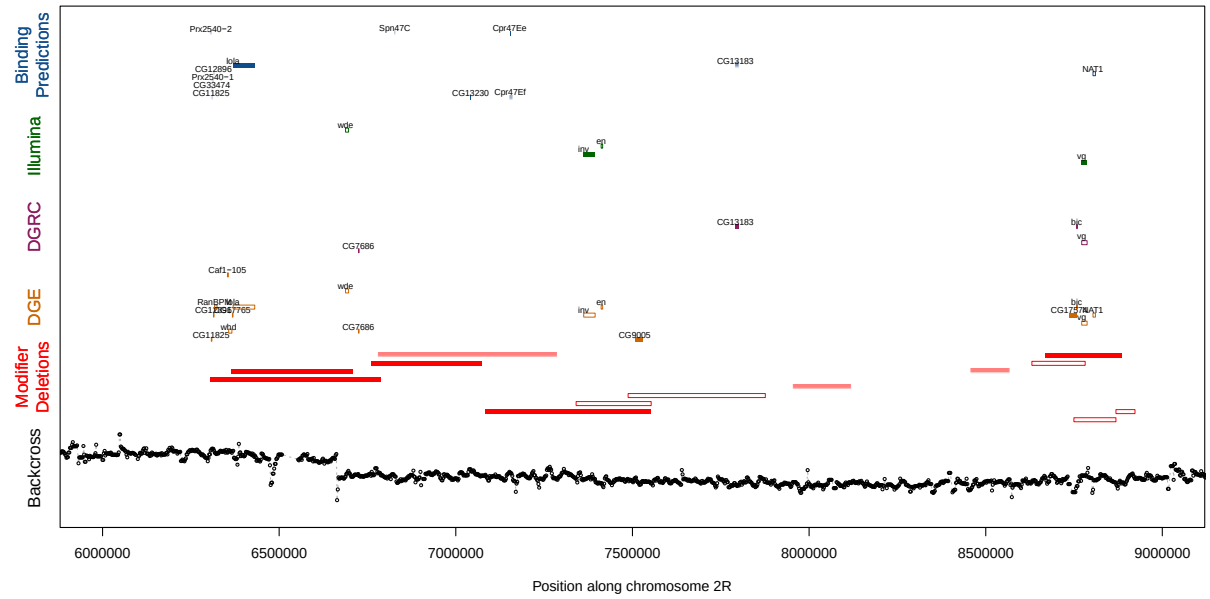
Binding Predictions
Illumina
DGRC
DGE
Modifier Deletions
Backcross
Prx2540−2
Spn47C
Cpr47Ee
lola
Prx2540−1
CG33474
CG11825
CG13230
Cpr47Ef
CG13183
NAT1
wde
inv
en
vg
CG7686
Caf1−105
bic
6000000
6500000
7000000
7500000
8000000
8500000
9000000
Position along chromosome 2R

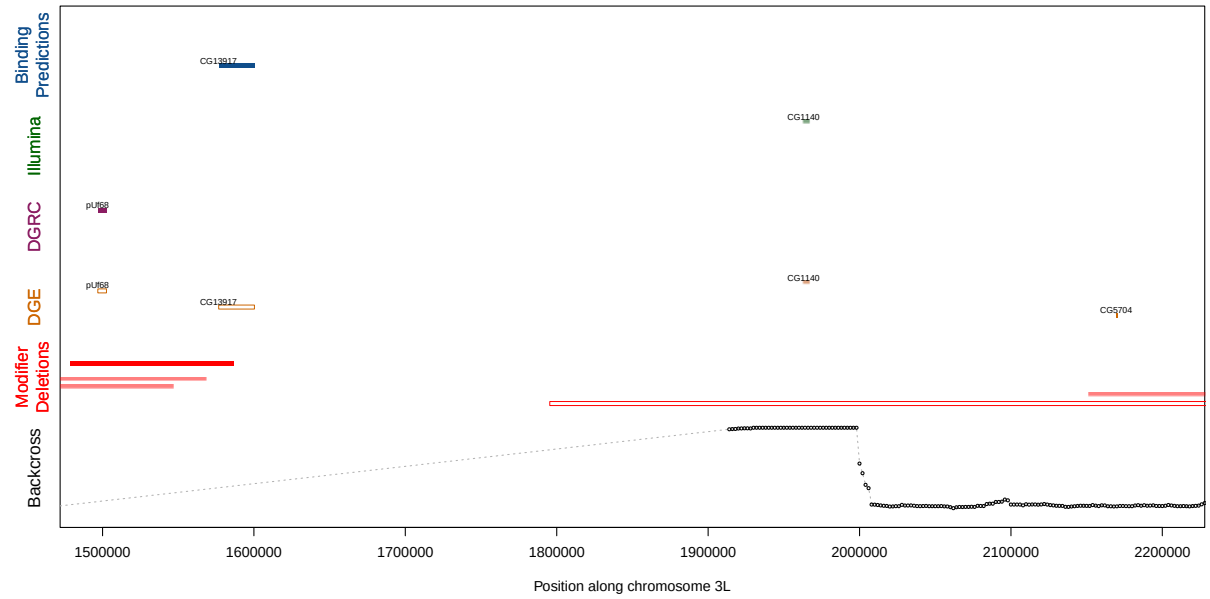
Binding Predictions
Illumina
DGRC
DGE
Modifier Deletions
Backcross
CG13917
CG1140
pUf68
CG5704
1500000
1600000
1700000
1800000
1900000
2000000
2100000
2200000
Position along chromosome 3L

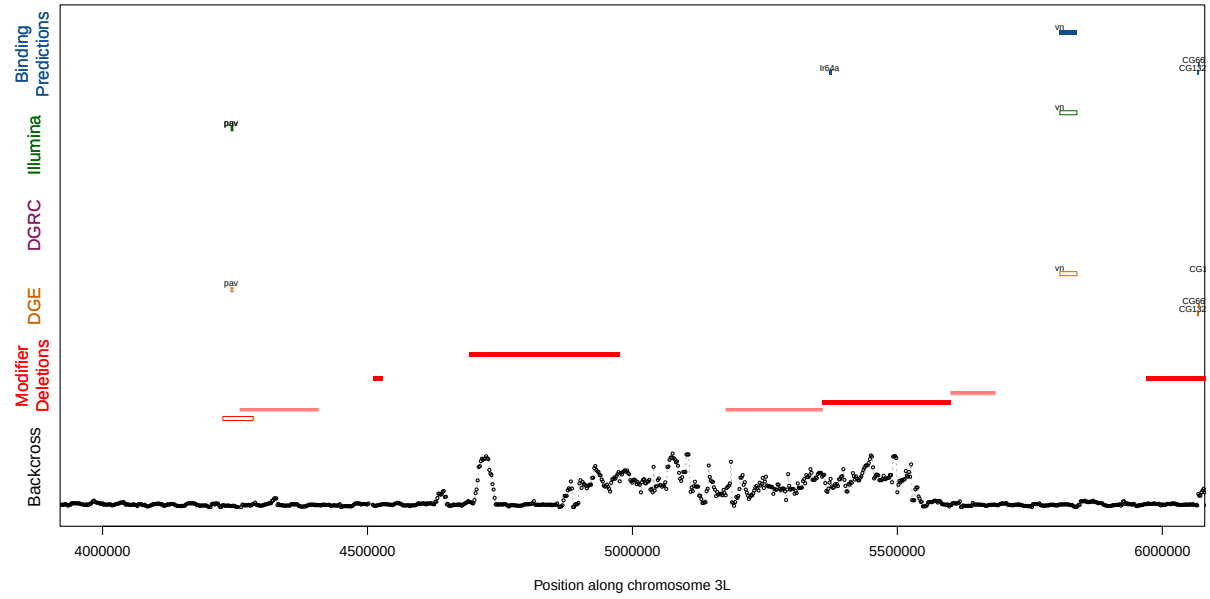
Binding Predictions
Illumina
DGRC
DGE
Modifier Deletions
Backcross
vn
Ir64a
pav
4000000
4500000
5000000
5500000
6000000
Position along chromosome 3L

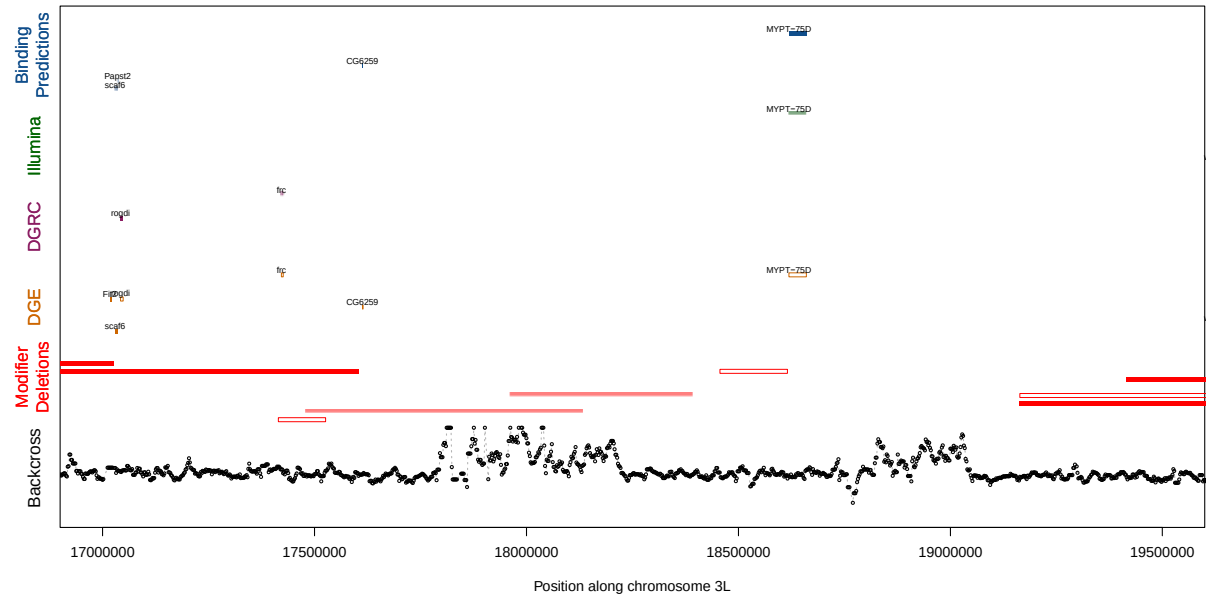
Binding Predictions
Illumina
DGRC
DGE
Modifier Deletions
Backcross
MYPT-75D
CG6259
Papst2
scaf6
frc
rogdi
17000000
17500000
18000000
18500000
19000000
19500000
Position along chromosome 3L

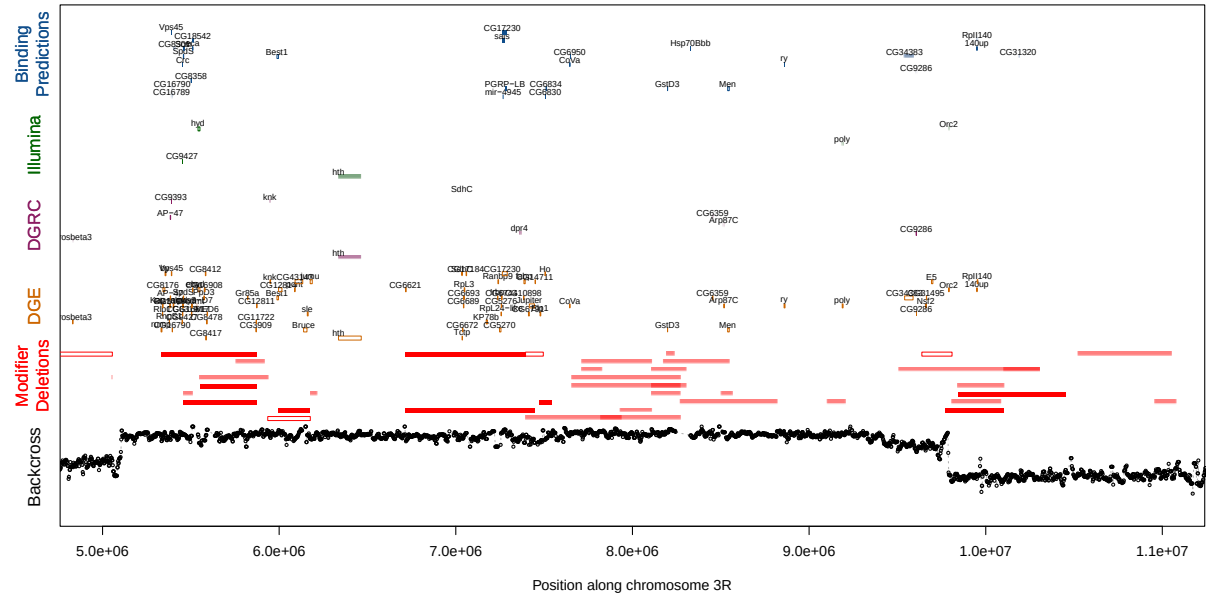
Binding Predictions
Illumina
DGRC
DGE
Modifier Deletions
Backcross
Best1
CG6950
CqVa
Hsp70Bbb
GstD3
Men
CG9286
Orp2
poly
CG9427
hth
SdhC
knk
dpr4
CG6359
Arpp87C
CG6621
Ptp
5.0e+06
6.0e+06
7.0e+06
8.0e+06
9.0e+06
1.0e+07
1.1e+07
Position along chromosome 3R

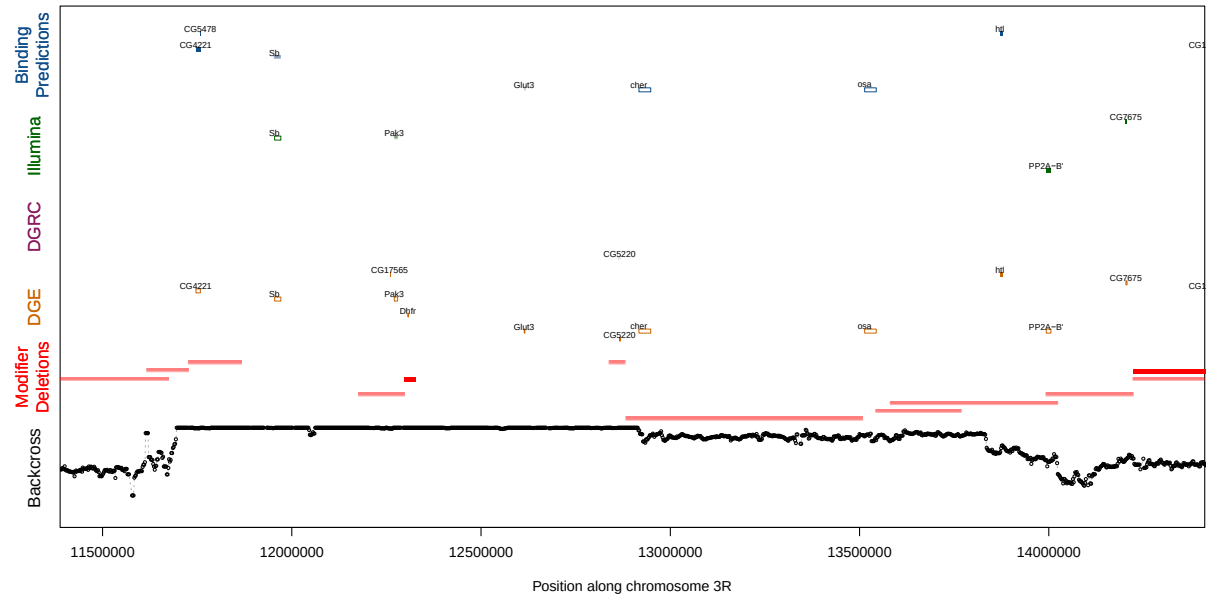

Figure S5 Integrated plots showing results of independent genomic datasets used to investigate the genetic basis of background dependence of the sd^{E3} phenotype. Backcross: Average frequency of the ORE (short-wing) allele across four short-wing introgression lines. Modifier deletions: open bars represent deletions with a significant main effect on the sd^{E3} phenotype; light shaded bars represent deletions with a significant background-dependent effect on the sd^{E3} phenotype; and dark shaded bars represent deletions in which both the main and interaction effects are significant. DGE: open bars represent genes whose transcript counts are influenced by *sd* genotype; light shaded bars represent genes showing evidence of genotype-dependent allelic imbalance; and dark shaded bars represent genes showing evidence of both an overall effect of *sd* genotype and genotype-dependent allelic imbalance. DGRC and Illumina: open bars represent genes showing evidence of an effect of *sd* genotype on expression; light shaded bars represent genes showing evidence of a genotype-by-background interaction effect; and dark shaded bars represent genes showing evidence of both the main and interaction effects. Binding predictions: open bars represent genes predicted to be overall SD binding targets (in at least one of the two genetic backgrounds); light shaded bars represent genes predicted to show differential affinity for SD between the two backgrounds; and dark shaded bars represent genes showing evidence of both overall SD binding and differential affinity between backgrounds. Only genes showing evidence of at least four significant effects across all datasets are shown.

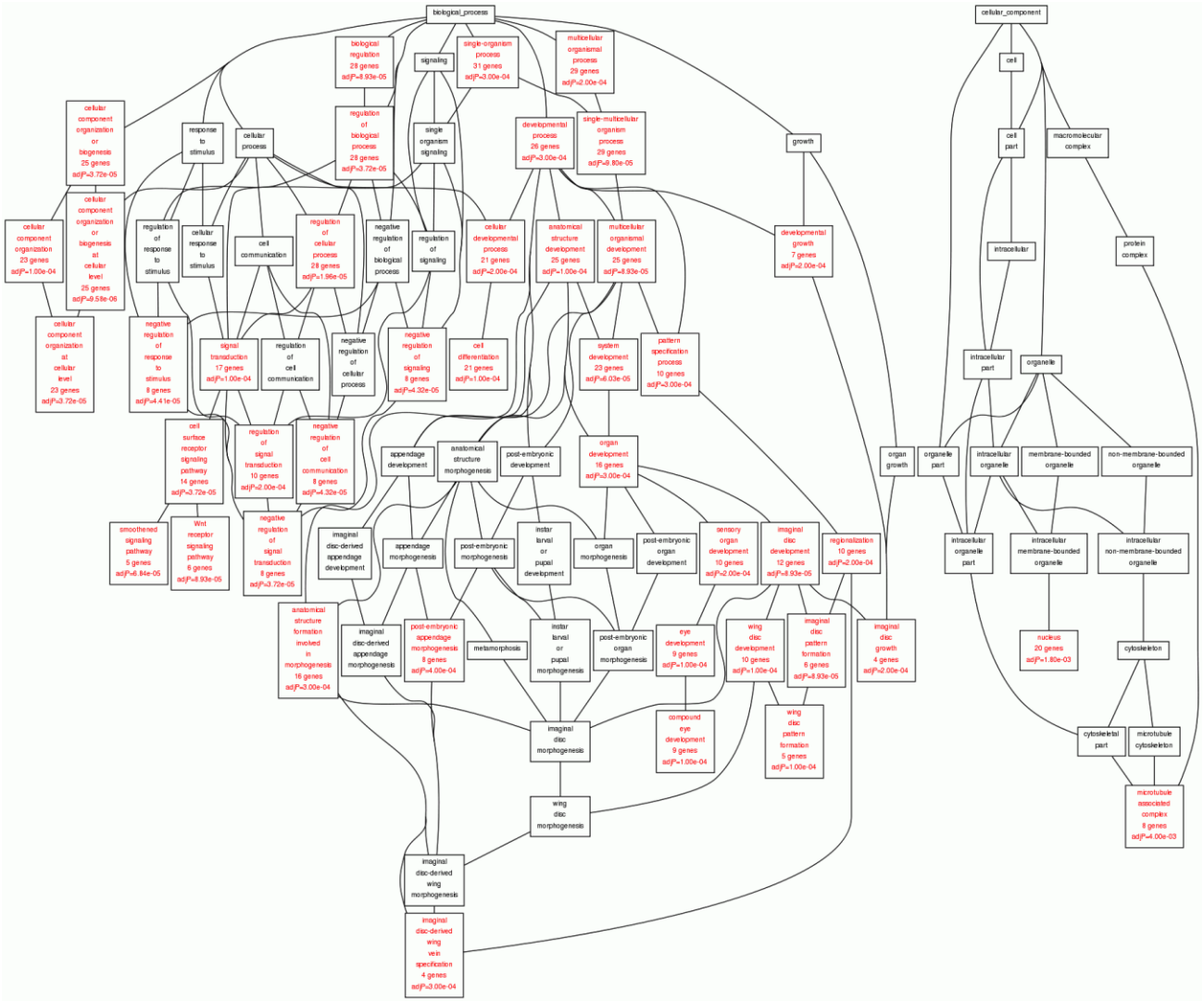
biological_process
biological regulation 28 genes adjP=8.93e-05
signaling
single-organism process 31 genes adjP=3.00e-04
multicellular organismal process 29 genes adjP=2.00e-04
cellular component organization or biogenesis 25 genes adjP=3.72e-05
response to stimulus
cellular process
regulation of biological process 28 genes adjP=3.72e-05
single organism signaling
developmental process 26 genes adjP=3.00e-04
single-multicellular organism process 29 genes adjP=8.80e-05
growth
cellular component organization or biogenesis 23 genes adjP=1.00e-04
cellular component organization or biogenesis at cellular level 25 genes adjP=9.59e-06
regulation of response to stimulus
cellular response to stimulus
cell communication
regulation of cellular process 28 genes adjP=1.98e-05
negative regulation of biological process
regulation of signaling
cellular developmental process 21 genes adjP=2.00e-04
anatomical structure development 25 genes adjP=1.00e-04
multicellular organismal development 25 genes adjP=8.93e-05
developmental growth 7 genes adjP=2.00e-04
cellular component organization at cellular level 23 genes adjP=3.72e-05
negative regulation of response to stimulus 8 genes adjP=4.41e-05
signal transduction 17 genes adjP=1.00e-04
regulation of cell communication
negative regulation of cellular process
negative regulation of signaling 8 genes adjP=4.32e-05
cell differentiation 21 genes adjP=1.00e-04
system development 23 genes adjP=6.03e-05
pattern specification process 10 genes adjP=3.00e-04
cell surface receptor signaling pathway 14 genes adjP=3.72e-05
regulation of signal transduction 10 genes adjP=2.00e-04
negative regulation of cell communication 8 genes adjP=4.32e-05
appendage development
anatomical structure morphogenesis
post-embryonic development
organ development 16 genes adjP=3.00e-04
organ growth
smoothened signaling pathway 5 genes adjP=6.84e-05
Wnt receptor signaling pathway 6 genes adjP=8.93e-05
negative regulation of signal transduction 8 genes adjP=3.72e-05
imaginal disc-derived appendage development
appendage morphogenesis
post-embryonic morphogenesis
instar larval or pupal development
organ morphogenesis
post-embryonic organ development
sensory organ development 10 genes adjP=2.00e-04
imaginal disc development 12 genes adjP=8.93e-05
regionalization 10 genes adjP=2.00e-04
anatomical structure formation involved in morphogenesis 16 genes adjP=3.00e-04
imaginal disc-derived appendage morphogenesis
post-embryonic appendage morphogenesis 8 genes adjP=4.00e-04
metamorphosis
instar larval or pupal morphogenesis
post-embryonic organ morphogenesis
eye development 9 genes adjP=1.00e-04
wing disc development 10 genes adjP=1.00e-04
imaginal disc pattern formation 6 genes adjP=8.93e-05
imaginal disc growth 4 genes adjP=2.00e-04
imaginal disc morphogenesis
compound eye development 9 genes adjP=1.00e-04
wing disc pattern formation 5 genes adjP=1.00e-04
wing disc morphogenesis
imaginal disc-derived wing morphogenesis
imaginal disc-derived wing vein specification 4 genes adjP=3.00e-04
cellular_component
cell
cell part
macromolecular complex
intracellular
protein complex
intracellular part
organelle
organelle part
intracellular organelle
membrane-bounded organelle
non-membrane-bounded organelle
intracellular organelle part
intracellular membrane-bounded organelle
intracellular non-membrane-bounded organelle
nucleus 20 genes adjP=1.80e-03
cytoskeleton
cytoskeletal part
microtubule cytoskeleton
microtubule associated complex 8 genes adjP=4.00e-03

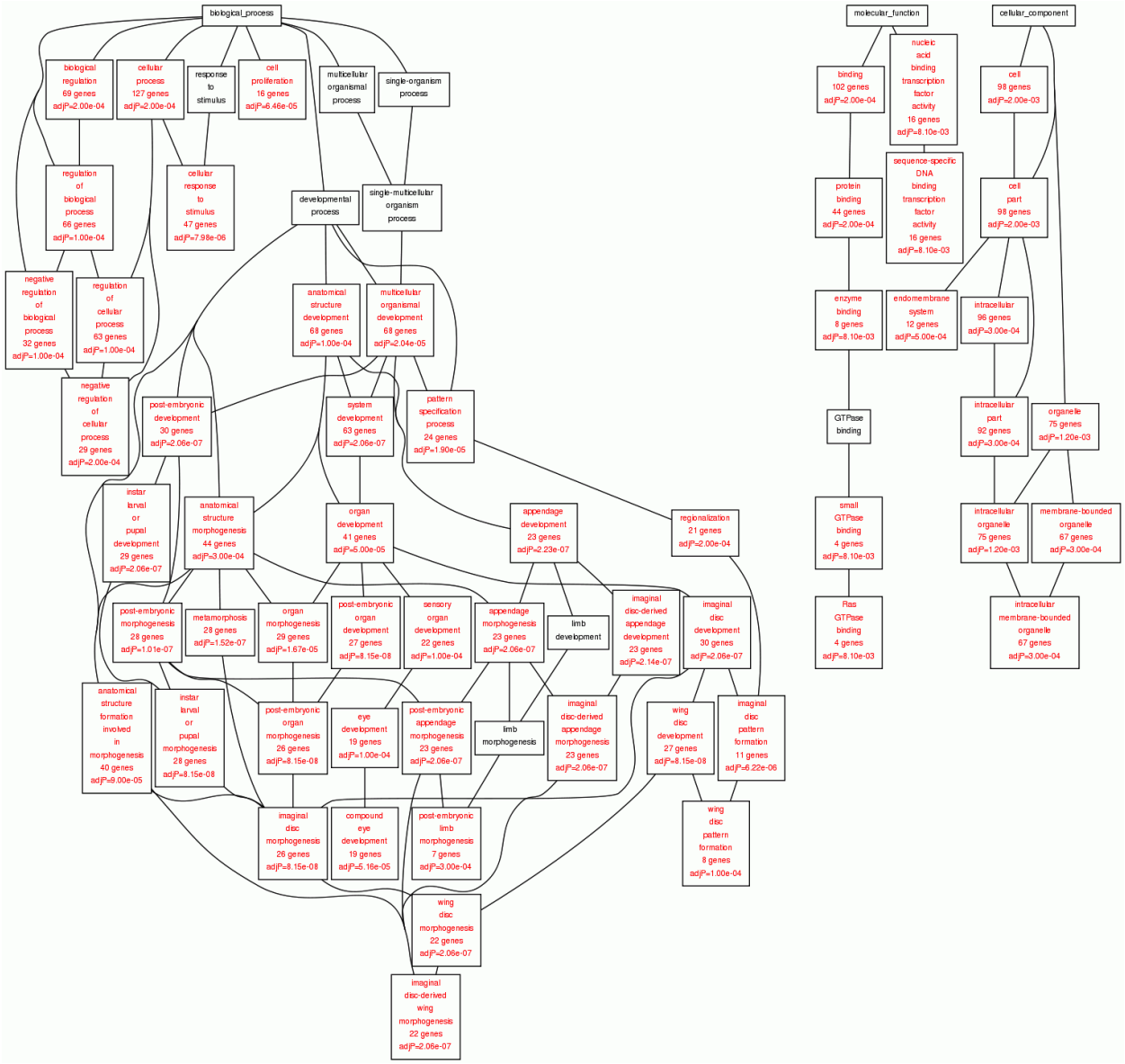

Figure S6 Top scoring GO hits for candidate genes identified by integrated analysis using (A) significant *sd* genotype effects for expression datasets and (B) significant genotype-by-background interaction effects for expression datasets.

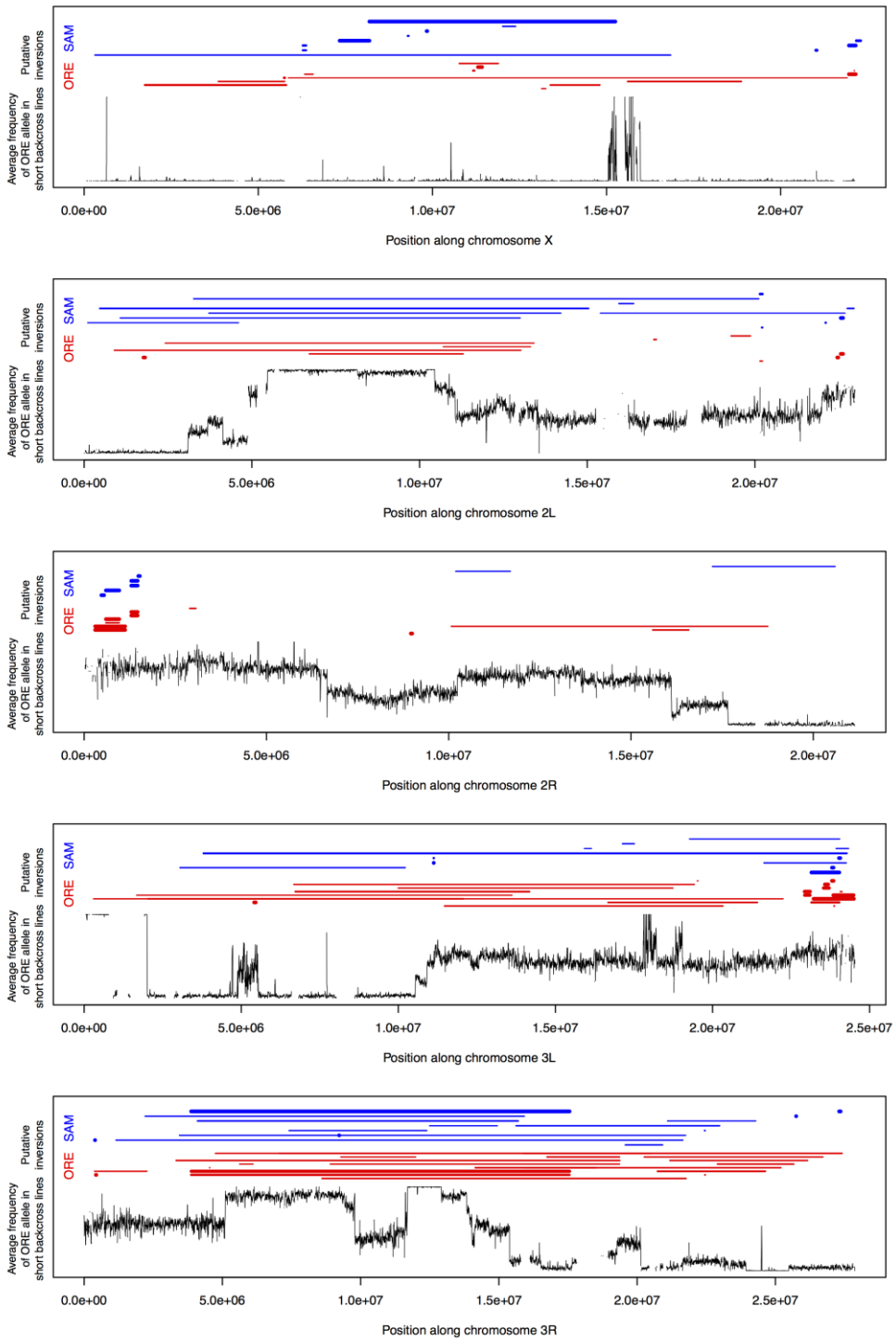

Figure S7 Weak evidence for putative inversions based on paired-end reads mapping to discordant locations in the genome. Thicker bars indicate stronger evidence. Inversions are relative to the *D. melanogaster* reference genome. We searched for inversions using BreakDancer v1.1 (Chen et al. 2009).

References

Bailey TL, Bodén M, Buske FA, Frith M, Grant CE, Clementi L, Ren J, Li WW, Nole WS: **MEME SUITE: tools for motif discovery and searching.** *Nucleic Acids Res* 2009, **37**:W202-W208.

Chen K, Wallis JW, McLellan MD, Larson DE, Kalicki JM, Pohl CS, McGrath SD, Wendl MC, Zhang Q, Locke DP, Shi X, Fulton RS, Ley TJ, Wilson RK, Ding L, Mardis ER: **BreakDancer: an algorithm for high-resolution mapping of genomic structural variation.** *Nat Methods* 2009, **6**:677-681.

Guss KA, Nelson CE, Hudson A, Kraus ME, Carrol SB: **Control of a genetic regulatory network by a selector gene.** *Science* 2001, **292**: 1164-1167.

Halder G, Carrol SB: **Binding of the Vestigial co-factor switches the DNA-target selectivity of the Scalloped selector protein.** *Development* 2001, **128**: 3295-3305.